



8-2016

The Use of Sodium Persulfate in Hydraulic Fracturing Fluids: A Degradation Study Based on Furfural

Katherine Elizabeth Manz

University of Tennessee, Knoxville, kmanz1@vols.utk.edu

Follow this and additional works at: https://trace.tennessee.edu/utk_gradthes

 Part of the [Environmental Chemistry Commons](#), [Environmental Engineering Commons](#), [Environmental Indicators and Impact Assessment Commons](#), [Oil, Gas, and Energy Commons](#), [Other Chemistry Commons](#), and the [Water Resource Management Commons](#)

Recommended Citation

Manz, Katherine Elizabeth, "The Use of Sodium Persulfate in Hydraulic Fracturing Fluids: A Degradation Study Based on Furfural. " Master's Thesis, University of Tennessee, 2016.
https://trace.tennessee.edu/utk_gradthes/4012

This Thesis is brought to you for free and open access by the Graduate School at TRACE: Tennessee Research and Creative Exchange. It has been accepted for inclusion in Masters Theses by an authorized administrator of TRACE: Tennessee Research and Creative Exchange. For more information, please contact trace@utk.edu.

To the Graduate Council:

I am submitting herewith a thesis written by Katherine Elizabeth Manz entitled "The Use of Sodium Persulfate in Hydraulic Fracturing Fluids: A Degradation Study Based on Furfural." I have examined the final electronic copy of this thesis for form and content and recommend that it be accepted in partial fulfillment of the requirements for the degree of Master of Science, with a major in Environmental Engineering.

Kimberly Carter, Major Professor

We have read this thesis and recommend its acceptance:

Chris Cox, Khalid Alshibli

Accepted for the Council:

Carolyn R. Hodges

Vice Provost and Dean of the Graduate School

(Original signatures are on file with official student records.)

**The Use of Sodium Persulfate in Hydraulic Fracturing
Fluids: A Degradation Study Based on Furfural**

A Thesis Presented for the
Master of Science
Degree
The University of Tennessee, Knoxville

Katherine Elizabeth Manz

August 2016

Copyright © 2016 by Katherine E. Manz

All rights reserved.

DEDICATION

To my late grandma, Katherine Neuber, who taught me all of “life’s important lessons” and for being the role model that I always admired and looked up to. Thank you for sparking my interest in science and teaching me that if you put your mind to it, you can accomplish anything.

To my late grandpa, John A. Manz, who helped open up the door for success in my education and my personal goals. Thank you for sharing your love and passion for science education with me.

ACKNOWLEDGMENTS

First, I would like to express my gratitude and sincerest appreciation to my advisor and mentor, Dr. Kimberly Carter. I would like to thank you for your extensive guidance, support, understanding, and encouragement in pursuing a Master's degree. The opportunity she gave me was more than I could have hoped for - I have gained so many valuable skills and experiences.

Next, I would also like to thank my committee members, Dr. Chris Cox and Dr. Qiang He. I really appreciate the enthusiasm, support, and feedback you have provided me with over the last few years.

Third, I would like to thank the undergraduate students, Jessica Lucchesi, Gregory Hearr, and Taylor Adams, who have helped me in the laboratory on this work. I would especially like to thank Taylor, for his dedication and determination with the pressurized reactor.

I would like to thank my family and friends. My parents, Rose and Joe, and brother, CJ, have always been my number one fans. I cannot express how grateful I am for your endless support in all of my endeavors. You have unceasingly believed in me and encouraged me. Your examples of hard work, persistence, and refusal to give up pushed me forward when I was ready to throw in the towel. Finally, I would like to thank Christopher, my love and best friend, thank you for your patience, understanding, and encouragement to pursue my goals and dreams.

ABSTRACT

Hydraulic fracturing has allowed natural gas to become a viable energy source via extraction of unconventional shale reserves, but this process requires an enormous amount of water. To ensure a productive fracture, a proprietary blend of chemical additives is added to the water. In this research, a hydraulic fracturing chemical additive – an enzyme breaking agent – is analyzed for organic components using gas chromatography mass spectrometry. The chemical changes that occur over the course of a fracture are also investigated using one model chemical found in the additive, furfural, in order to help assess the environmental risk that hydraulic fracturing poses. This is done by studying furfural's interactions with sodium persulfate, which is added to hydraulic fracturing fluids as an oxidizing breaking agent. Sodium persulfate is also used as a powerful disinfectant for the treatment of groundwater contamination. Once activated, sodium persulfate reacts to form sulfate radicals. Various conditions may be used to activate persulfate in order to increase the rate of sulfate radical production, including temperature and the presence of iron. This study focuses on the use of Fe (III) and the influence of temperature, initial pH, initial persulfate dose, iron concentration, hydraulic fracturing brine, and elevated pressure on the kinetics of furfural degradation. The goal of this research is to determine the efficiency and optimal conditions necessary for employing sodium persulfate as a treatment option for furfural contamination and the identification of reaction byproducts. Kinetic parameters, including pseudo first-order reaction rate constants and activation energies, are presented.

TABLE OF CONTENTS

Chapter 1: Introduction	1
Chapter 2: Literature Review	4
Chapter 3: Research Objectives	9
Chapter 4: Materials and Methods	10
4.1. Chemicals	10
4.2. Experimental procedures	10
4.2.1. Batch experiments at ambient pressure	10
4.2.2. Experiments using pressurized reactor	11
4.2.3. Furfural analysis	12
4.2.4. “LEB10-X” and reaction byproduct analysis	12
Chapter 5: Results and Discussion	14
5.1. GC/MS analysis of LEB-10X	14
5.2. Kinetic modeling and furfural persistence	14
5.3. Furfural oxidation via sodium persulfate in water	16
5.3.1. Temperature effects	16
5.3.2. Effect of pH	22
5.3.3. Effect of initial persulfate dose	24
5.3.4. Effect of iron concentration	24
5.3.5. Byproduct identification and pathway discussion	29
5.4. Furfural degradation via sodium persulfate in hydraulic fracturing conditions	31
5.4.1. Effect of temperature and Arrhenius model	31
5.4.2. Effect of brine pH	34
5.4.3. Effect of initial persulfate dose	37
5.4.4. Overall impact of hydraulic fracturing brine on kinetics	37
5.4.5. Byproduct identification in hydraulic fracturing brine	40
5.6. Furfural degradation at elevated pressure	44
Chapter 6: Conclusions	47
References	48
Appendix	55
Vita	62

LIST OF TABLES

Table 1. Chemical composition of hydraulic fracturing brine used in this study.	11
Table 2. Pseudo first-order reaction rate constants for furfural oxidation via activated persulfate.	20
Table 3. Arrhenius parameters for furfural removal.	22
Table 4. Pseudo first-order reaction rate constant of furfural degradation in the presence of hydraulic fracturing brine.	32
Table 5. Arrhenius parameters in the presence of hydraulic fracturing brine.	34

LIST OF FIGURES

Figure 1. Gas chromatogram and mass spectrum of LEB-10X.....	15
Figure 2. Half-life of furfural in water, hydraulic fracturing brine, and hydraulic fracturing brine with 23.33 mg L ⁻¹ ferric sulfate (no sodium persulfate added).....	16
Figure 3. The decrease in furfural concentration over the course of 480 minutes with (a) 0 mg L ⁻¹ (b) 23.33 mg L ⁻¹ ferric sulfate. The initial pH was 5.4 and the initial dose of sodium persulfate was 21 mM.....	18
Figure 4. Arrhenius plots for the oxidation of furfural by sodium persulfate with 0 and 23.33 mg L ⁻¹ ferric sulfate with an pH of a) 2.54 and b) 5.4.	19
Figure 5. Influence of pH on the reaction rate constant of furfural degradation with 0 mg L ⁻¹ ferric sulfate and at 55°C.	23
Figure 6. Effect of persulfate dose on the concentration of furfural at 55°C at pH 5.4 with (a) 0 mg L ⁻¹ ferric sulfate and (b) 23.33 mg L ⁻¹ ferric sulfate.	25
Figure 7. Relationship between the initial concentration of persulfate and the reaction rate constant at 55°C and pH 5.4 with 0 and 23.33 mg L ⁻¹ ferric sulfate.	26
Figure 8. Effect of iron concentration on furfural degradation over time at 55°C, pH 5.4, and initial persulfate dose of 15 mM.	27
Figure 9. Comparison of the use of Fe(III) and Fe(II) to activate persulfate for furfural removal (pH 5.4, T = 55°C, initial persulfate dose = 15 mM).....	28
Figure 10. Proposed reaction pathway.....	30
Figure 11. The effect of temperature on furfural degradation in the presence of hydraulic fracturing brine. Experimental conditions: pH 2.54, 21 mM dose of sodium persulfate, and a) 0 mg L ⁻¹ ferric sulfate and b) 23.33 mg L ⁻¹ ferric sulfate.....	33
Figure 12. Arrhenius plot of furfural degradation in the presence of hydraulic fracturing brine with and without ferric sulfate (pH 2.54, initial sodium persulfate dose of 21 mM).	35
Figure 13 . Effect of initial pH – a) 5.4, b) 2.54 – of the hydraulic fracturing brine at different doses of sodium persulfate (55°C).....	36
Figure 14. The initial dose of persulfate has an effect on furfural removal with a) 0 mg L ⁻¹ ferric sulfate and b) 23.33 mg L ⁻¹ ferric sulfate. The effect of persulfate dose on pseudo-first order reaction rate constant is shown in c) with and without ferric sulfate.....	38

Figure 15. Furfural removal (pH 2.54) in water and a) 0 and b) 23.33 mg L ⁻¹ ferric sulfate and in hydraulic fracturing brine with c) 0 and d) 23.33 mg L ⁻¹ ferric sulfate at different temperatures.	39
Figure 16. Effect of having brine in solution on the pseudo first-order reaction rate constant (55°C, 23.33 mg L ⁻¹ ferric sulfate).	41
Figure 17. Comparison of all established activation energies.	42
Figure 18. Reaction byproducts of furfural oxidation in the presence of hydraulic fracturing brine.	43
Figure 19. Activation energy for furfural removal with 0 and 3,000 psi applied to the reactor.	46
Figure A 1. Flow diagram of the pressurized reactor used in this study.	56
Figure A 2. Pressurized reactor set-up.	57
Figure A 3. The influence of varying pH on the degradation of furfural via persulfate oxidation with (a) 0 mg L ⁻¹ ferric sulfate and 5 mM sodium persulfate, (b) 0 mg L ⁻¹ ferric sulfate and 10 mM sodium persulfate, (c) 0 mg L ⁻¹ ferric sulfate and 15 mM sodium persulfate, (d) 23.33 mg L ⁻¹ ferric sulfate and 5 mM sodium persulfate, (e) 23.33 mg L ⁻¹ ferric sulfate and 10 mM sodium persulfate, and (f) 23.33 mg L ⁻¹ ferric sulfate and 15 mM sodium persulfate.	58
Figure A 4. Mass spectra of a bromoform standard and the bromoform detected in a hydraulic fracturing fluid sample.	59
Figure A 5. Furfural removal over time in the high pressure reactor without applied pressure.	60
Figure A 6. Furfural removal over time in the high pressure reactor with 3,000 psi applied.	61

NOMENCLATURE

A	Frequency, or collision, factor
AOP	Advanced oxidation process
DBPs	Disinfection byproducts
E_a	Activation energy
E°	Electric potential
Fe_2SO_4	Ferric sulfate, Fe (III)
$FeSO_4$	Ferrous sulfate, Fe (II)
GC/MS	Gas chromatography mass spectrometry
HAAs	Halogenated acetic acids
HANs	Haloacetonitriles
$HO\cdot$	Hydroxyl radical
ISCO	In situ chemical oxidation
k_{obs}	Observed pseudo first-order rate constant
LEB10-X	Hydraulic fracturing enzyme breaking agent
$Na_2S_2O_8$	Sodium persulfate
R	Universal gas constant
$S_2O_8^{2-}$	Persulfate anion
$SO_4^{\cdot-}$	Sulfate radical
$t_{1/2}$	Half-life
TDS	Total dissolved solids
THMs	Trihalomethanes
UV	Ultraviolet light

CHAPTER 1: Introduction

Although water covers the majority of the earth's surface, the demand for this resource is extremely high. While water supply is a global concern, due to recent events in the United States, such as the California drought – deemed an “exceptional” drought by the US drought monitor, the demand for clean water in the US is higher than ever [1]. As the water supply problem continues to increase, demands from population and energy production continue to increase. In response to the energy demand, the US has been searching for ways to become energy independent and to increase energy security. To achieve this goal, the US has turned to natural gas as a viable energy source [2]. Meeting the demand for natural gas has been achieved through extraction from wells of shale rock approximately 1 mile below the earth's surface via hydraulic fracturing [3]. Recently, hydraulic fracturing has become of public concern due to its impacts on the environment and practices set forth by the oil and gas industry.

Hydraulic is not a new technology and has significant environmental impacts on water, land, and air quality. It was invented in 1947 by Floy Ferris of Stanolind Oil and Gas [4]. However, recent advancements in this technology have made it more productive and efficient allowing companies to go from vertical wells to the now more common horizontal wells. Given that the shale layer is wider than it is thick, horizontal drilling enables drilling in multiple directions, increasing productivity. Horizontal drilling requires two to ten million gallons of water per well fractured, which puts an enormous strain on regions with limited water supply [5, 6]. On average, the US used 44 billion gallons of water per year for hydraulic fracturing in 2011 and 2012 [7]. In a recent report published by Ceres, of all the wells hydraulically fractured since 2011, 47% were in regions of high or extremely high water stress [8].

The fluid injected into the well is a “chemical slurry,” containing 200,000 liters of chemical additives, 98 to 99% water, and 1 to 2% proppant [9, 10]. The chemical additives and their concentration used vary depending on the shale formation, location of the fracture, the company performing the fracture, and the day-to-day conditions at the well-pad, such as temperature. The additives have a variety of purposes - friction reducers, gelling agents, breaking agents, biocides, scale inhibitors, clay stabilizers, corrosion inhibitors, surfactants, and proppants. Once fluid

injection is completed, about 60% of the original volume is returned to the surface of the well in the “flowback” stage. The “flowback” fluids are the fluids that return to the surface prior to production over a ten-day period. The “produced” water stage occurs once the well has been put into production and the amount of water returning to the surface can total 10 to 300% of the injected volume. These fluids returning to the surface contain the remaining proppants and chemical additives as well as fluids and materials extracted from the geological formation, known as “brine.” The brine introduces high concentrations of inorganic and organic salts, or total dissolved solids (TDS) to the wastewater [11].

Instances where hazardous hydraulic fracturing fluids leak into groundwater via breaks in the cement casings have been reported, but spills most commonly occur when transporting the fluids or when filling and emptying storage tanks [12]. These spills contaminate the groundwater with the chemical additives and species extracted from the shale formation. Colborn *et al.* associated 71 chemicals detected in hydraulic fracturing fluids with 10 or more health risks and toxicity in concentrations less than one part per million [13]. Of the chemicals known to be used in hydraulic fracturing, 75% are known skin, eye, and sensory organ irritants; 25% are known carcinogens, many cause reproductive, mutagenic, kidney, immune system, or respiratory effects; and many have no safety information associated with them [13]. The TDS in hydraulic fracturing wastewater has been shown to be persistent – in North Dakota, elevated levels of contaminants from spills have been detected for four years [12]. This may have a severe impact on the ecosystem surrounding a spill. Bamberger *et al.*, have shown the severe impact of exposing livestock, pets, horses, and even humans to hydraulic fracturing fluids – in the most extreme case, 17 cows were killed within one hour of exposure to hydraulic fracturing wastewater [14]. Despite the increasing awareness of the fluid toxicity, supporters of hydraulic fracturing companies argue that these substances are non-toxic for the most part or that they are using them at such low concentrations that they cause no harm [15].

The overall impacts of hydraulic fracturing are not well understood or agreed upon by all scientists [16]. Hydraulic fracturing has significantly reduced the price of fossil fuels in the US and it is predicted by the Energy Information Administration that hydraulic fracturing will continue to expand [2]. It is our responsibility for future generations to gain a better understanding of the

underlying science and environmental impacts of hydraulic fracturing. In order to clearly explain the nature of the problem and the environmental risk hydraulic fracturing poses, the chemistry of the fluids injected into the well and the life-cycle of these fluids, including the changes in the fluids before and after a fracture, must be understood. Therefore, in this work, the chemical changes that occur over the course of a fracture are investigated using one model chemical additive, furfural – a component of the hydraulic fracturing enzyme breaking agent.

CHAPTER 2: Literature Review

One chemical additive used in hydraulic fracturing fluids is furfural, or 3-furaldehyde, as a coating polymer for proppants [17-19]. Furfural is an oily compound with an almond-like odor. It has a furan derived structure and is highly resistant to heat, acid, and water [20]. Furfural has gained attention due to potential use as a building block for hydrocarbon fuels [21]. The chemical is produced through the decomposition of plant biomass, such as bran used to make cereal, through acid-catalyzed digestion of pentose sugars [22]. Furfural is used as a preservative, fungicide, herbicide, disinfectant, as a precursor for many other compounds and synthetic resins, and as demulsifying agent in petroleum refining [23, 24]. However, furfural has been found to have toxic and inhibitory effects on both aerobic and anaerobic biological processes by decreasing specific growth rate and ethanol production [25-27]. Furfural has been shown to be toxic to human health, primarily effecting the skin, liver, and kidneys [28]. The Occupational Safety and Health Administration (OSHA) permissible exposure limit for skin contact is 5 ppm over an eight-hour time weighted average [29].

In order to remove furfural from water, many industries use steam extraction [30]. This process consumes a significant amount of water to produce the required 18 to 25 tons of steam needed to recover 1 ton of furfural. Overall, the process only recovers 60% of the furfural while 40% remains in the condensed steam water and may be released into the environment [30]. Another method used to remove furfural from water is adsorption with commercial grade activated carbon (AAC), granular activated carbon (GAC), zeolites, nanoporous silica based MCM-48 material, and polymeric resins [31-37]. Of these adsorption techniques, diffusion coefficients, or the rate of material transport as a result of diffusion, were given for AAC and GAC, and were $3.34 \times 10^{-13} \text{ m}^2/\text{s}$ and $9.870 \times 10^{-10} \text{ m}^2/\text{s}$, respectively [31, 32]. Groundwater remediation using these methods require pump and treat technology, which can be expensive to design, install, operate, and maintain [38].

A potential alternative method for removing furfural from contaminated groundwater is using *in situ* chemical oxidation (ISCO), or advanced oxidation processes (AOPs), via activated persulfate. Persulfate continues to gain attention over other ISCO agents because it does not decay rapidly, it does not harm native microorganisms, and it produces very strong oxidizing radicals

[39]. Of the commercially available persulfate salts (ammonium, sodium, and potassium), sodium persulfate has the greatest solubility (73g/100g H₂O at 25°C) and is the most stable at 25°C, making it the most preferable for ISCO in the field [40]. In addition, hydraulic fracturing companies use sodium persulfate as a breaking agent in order to decrease fluid viscosity by decomposing the gelling agents [41]. The concentration of sodium persulfate used depends on the conditions of the fracture, but concentrations as low as 0.125 mmol L⁻¹ up to as much as 47 mmol L⁻¹ have been reported [4, 42-44].

The persulfate anion has an oxidation potential (E⁰) of 2.01 V. However, once activated, persulfate forms the more powerful sulfate radical (E⁰ = 2.7 V) as seen in Reactions 2.1, 2.2, and 2.3 below [45, 46]. Persulfate activation occurs through metals, especially iron, heat, ultraviolet (UV) light, acidic conditions, or a combination of these activators.



Persulfate has also been activated using the Meⁿ⁺¹ form of the transition metals manganese and iron, as shown in Reactions 2.4 [47, 48]. When Fe (III) is used, a persulfate radical and Fe(II) are generated. The Fe (II) produced may further react with persulfate anions as shown in Reaction 2.2. The persulfate anion radical can further oxidize organic contaminants.



Under certain conditions, additional oxidants may form. In acidic conditions, hydrogen peroxide forms as shown in Reaction 2.5. In the presence of iron, hydrogen peroxide (E⁰ = 1.77 V) reacts with the iron (III) to produce a hydroperoxyl radical (E⁰ = 1.44 V) and iron (II) as shown in Reaction 2.6. Subsequently, iron (II) reacts with hydrogen peroxide to form the hydroxyl radical, one of the most powerful oxidizing agents (E⁰ = 2.81 V) as seen in Reaction 2.6 [49, 50].

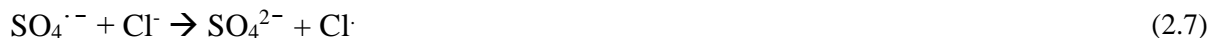


Several AOPs have shown success in degrading furfural, including UV, UV/H₂O₂, UV/H₂O₂/O₂, UV/H₂O₂/ Fe²⁺, UV/O₂/ Fe²⁺, O₃, UV/O₃, UV/TiO₂, and electrochemical methods [51-53]. Of the processes listed, the electrochemical method using 1.23 A of current and four iron electrodes removed the most furfural in the least amount of time (greater than 95% within 60 minutes) [51]. This process was followed by UV/H₂O₂ and UV/TiO₂, which both achieved greater than 95% furfural degradation within 2 hours. The methods used to stimulate hydrogen peroxide oxidation are similar to activation methods used for persulfate and both are typically activated in the field [54]. However, there are several advantages to using persulfate over hydrogen peroxide, including overall greater contaminant removal [54, 55]. Sodium persulfate has a higher oxidation potential than hydrogen peroxide and can generate a broader range of highly reactive radical intermediates [55-57]. Persulfate is stable and may be purchased in the solid form, whereas hydrogen peroxide is liquid and has the potential to explode when heated [40, 58]. Compared to the hydroxyl radical, which is produced during oxidation via hydrogen peroxide, the sulfate radical is able to transport greater distances in the sub-surface due to its stability [59]. Groundwater remediation using persulfate may also be performed without pump and treat methods, whereas methods requiring UV radiation would require to pump and treat.

The circumstances faced in hydraulic fracturing provide adequate conditions for persulfate activation. Over the course of a fracture, temperatures exceed 140°C and pressures can exceed 6,000 psi [60]. The dissolved iron content in hydraulic fracturing fluids can range between 0.1 and 222 mg L⁻¹, while total iron can range between 2.6 and 321 mg L⁻¹ [61]. Iron can exist in three oxidation states, 0, 2+ and 3+. In one study, flowback water quality was examined and determined to have a total iron content of 16 mg L⁻¹ and Fe²⁺ content below the detection limits of the study (0.2 mg L⁻¹) [62]. This suggests that, in these flowback fluid samples, the predominant oxidation state of iron is either Fe (0) or Fe (III).

Anions, especially carbonate, bicarbonate, and chloride, have been shown to have a negative impact on contaminant removal via heat-activated persulfate, but this impact is dependent on concentration and solution pH [63, 64]. Chloride and carbonate species have shown more pronounced scavenging effects on persulfate oxidation at basic pHs, rather than at pH's less than 7 [63, 65]. When these ions are present, less contaminant removal is achieved because they

compete for the sulfate radical. Chloride ions scavenge radicals by reacting with the persulfate radical and then with water, as seen in Reactions 2.7, 2.8 and 2.9 [63, 66, 67]. Carbonate species scavenge sulfate radicals by reacting directly with the sulfate radical as seen in Reactions 2.10, 2.11, and 2.12.



The presence of hydraulic fracturing brine could exhibit these sulfate radical scavenging effects and decrease the degree of organic content removal during groundwater remediation using persulfate. The TDS content of hydraulic fracturing wastewater ranges between 5,000 mg L⁻¹ to greater than 200,000 mg L⁻¹ and typically contains bromide, chloride, and metals, such as strontium and barium [11, 12, 68, 69]. The exact concentration of each brine constituent varies from one fracture to another; however, the brine may contain 32,000 to 148,000 mg L⁻¹ chloride, 720 to 1,600 mg L⁻¹ bromide, and 9,100 to 55,000 mg L⁻¹ carbonate species [11, 15, 70-72].

Due to the high levels of halogens, especially chloride and bromide, in hydraulic fracturing fluids, it is suspected that disinfection byproducts (DBPs), including trihalomethanes (THMs), haloacetic acids (HAAs) and haloacetonitriles (HANs), form in flowback fluids [73, 74]. As the DBPs are carcinogenic, they are regulated by the US Environmental Protection Agency (EPA) in drinking water [75]. It has also been shown that during disinfection treatment of hydraulic fracturing fluids diluted as low as 0.03% through chlorination, chloramination, and ozonation that DBPs form [73].

Like the previously mentioned disinfectants, persulfate is an oxidizing agent and has the potential to form DBPs in the presence of halogens. During the treatment of humic acid with heat activated-persulfate in a solution containing bromide ions, bromoform and bromoacetic acid were

detected [76]. When the halogens chloride, bromide, and iodide are all present in solution, UV activated persulfate oxidation of organic content in groundwater and surface water also resulted in the formation of THMs, HAAs, and HANs [77]. Brominated DBPs were the most prevalent, even though the bromide ion concentration was in the 30 to 100 μL^{-1} range and the chloride ions concentration was 4 mg L^{-1} . While DBP formation is an unintended consequence of water treatment, they have been associated with cancer, birth defects, cytotoxicity, genotoxicity, and many more adverse health effects [78]. It is important to assess the potential for DBP formation in persulfate oxidation using amounts that hydraulic fracturing companies add to the fluids as a breaking agent and in amounts that would typically be used to treat groundwater pollution from hydraulic fracturing spills.

This research examines the components of one hydraulic fracturing chemical additive called “LEB-10X,” a enzyme breaking agent, using gas-chromatography mass spectrometry (GC/MS). We identified furfural as a contaminant of interest and investigated furfural’s interactions with sodium persulfate, an oxidizing breaking agent, in hydraulic fracturing and non-hydraulic fracturing environments. Reactions in “hydraulic fracturing environments” were performed at conditions mimicking those faced in a fracture – in hydraulic fracturing brine, at various temperatures, at different pHs, and at elevated pressures. Reaction byproducts in in hydraulic fracturing and non-hydraulic fracturing environments were also identified using GC/MS.

CHAPTER 3: Research Objectives

The objectives of this work are to:

- Identify small organic molecules in an enzyme breaking agent called “LEB-10X,”
- Establish the persistence of furfural in water and in hydraulic fracturing brine,
- Evaluate the feasibility of heat-activated sodium persulfate for furfural removal,
- Determine the optimal conditions for furfural removal through persulfate ISCO,
- Identify reaction byproducts of furfural ISCO via sodium persulfate in water,
- Assess the impacts of using sodium persulfate as a hydraulic fracturing breaking agent and as a treatment option for groundwater pollution by hydraulic fracturing spills,
- Establish how hydraulic fracturing conditions, including high temperature, pressure, brine and iron presence, impact furfural ISCO, and
- Investigate what furfural transforms into as a consequence of persulfate oxidation in the presence of hydraulic fracturing brine.

CHAPTER 4: Materials and Methods

4.1. Chemicals

All solutions were prepared using deionized water produced using a Milli-Q Plus water purification system (Darmstadt, Germany). Furfural was purchased from Sigma Aldrich (St. Louis, MO 63103). Optima grade hexane and 97% tribromomethane stabilized with ethanol were purchased from Fisher Scientific (Pittsburgh, PA 15275, USA). Inorganic salts, aluminum sulfate (>99%), ferric sulfate (99%), hydrochloric acid, potassium bromide (>99%), potassium chloride (99%), potassium sulfate (99%), sodium bicarbonate (>99%), sodium hydroxide, sodium persulfate (>98%), and sodium chloride (>99%), were purchased from Fisher Scientific (Pittsburgh, PA 15275, USA). LEB-10X was obtained from Weatherford International (Houston, Texas, USA).

4.2. Experimental procedures

4.2.1. Batch experiments at ambient pressure

Furfural solutions were prepared 24 hours prior to starting the experiment and mixed using a magnetic stir bar. Solution pH was measured with a Fisher Scientific Accumet XL600 benchtop meter (Pittsburgh, PA 15275, USA) and adjusted to 2.54, 5.4, or 10.4 using sodium hydroxide or hydrochloric acid. Hydrochloric acid was added so that the volume was equal to 0.07% of the total volume, as done in the hydraulic fracturing industry [79]. This resulted in a final pH of 2.54, so all acidic solutions were adjusted to this pH. For experiments in brine solution, the constituents shown in were added and mixed at least overnight.

All experiments were carried out in triplicate using 125 mL capped amber borosilicate VOC (volatile organic carbon) bottles with Teflon-lined screw caps containing 100 mL of the furfural solution. The jars were set in a shaking water bath at 20, 30, 40, 55, and 60 °C at least 12 hours prior to the addition of sodium persulfate (New Brunswick Scientific Co, Inc, Model G76, Edison, NJ USA). Sodium persulfate stock solutions (1050 mM) were prepared 1 hour prior to the reaction. The reaction was initiated by spiking each amber jar with the appropriate volume of sodium persulfate solution at the beginning of the experiment. Oxidation controls, which were not spiked with sodium persulfate, were prepared in triplicate and furfural concentration stayed

constant over the course of the experiments. At each sampling time (0, 5, 10, 15, 30, 60, 90, 120, 180, 240, 360, 480 minutes), 4.5 mL of solution was collected using a pipette and placed in Eppendorf tubes resting on an ice bath. The Eppendorf tubes were placed in the ice bath in order to quench the oxidation reaction caused by residual persulfate. The samples were immediately placed in the freezer until further analysis. Samples were analyzed within 12 hours of collection.

Table 1. Chemical composition of hydraulic fracturing brine used in this study.

Brine Constituent	Concentration (mg L⁻¹)	Reference
Sodium Chloride	1,000	[11, 15, 70, 71]
Potassium Chloride	19.9	[15, 70, 72]
Potassium Sulfate	24.9	[70, 71]
Potassium Bromide	14.9	[11, 70, 72]
Sodium Bicarbonate	15.1	[70-72]
Ferric Sulfate	23.3	[11, 70, 71]
Aluminum Sulfate	14.9	[70-72]
TDS	1,104	

4.2.2. Experiments using pressurized reactor

High pressure experiments were conducted using an extra capacity high pressure generator purchased from HiP (Model 112-5.75-5, Erie, PA 16505 USA). A flow diagram of the experimental set-up and pictures of the reactor may be found in the Appendix, Figures A 1 and A 2. Reactions were performed in a 500 mL capacity O-ring seal reactor purchased from HiP (Model OC-9, Erie, PA 16505 USA). A custom-made silicone impregnated fiberglass heating jacket equipped with a programmable temperature controller purchased from HTS/Amptek was used to control the temperature of the reactor (Stafford, TX 77497). Experiments were performed at with no pressure applied to the reactor and 3,000 psi applied pressure. A reservoir was used to feed the reactor with a concentrated solution of 128 mM sodium persulfate. Each time a sample was collected the volume removed was replaced with the stock persulfate solution so that the concentration of persulfate inside the reactor was 5.12 mM. In order to keep the concentration of

persulfate consistent from experiment to experiment, samples were taken at 0, 5, 15, 20, 25, 30, 40, 50, 60, 75, 90, and 105 minutes in 20 mL volumes. For experiments performed at 20°C in the reactor, the experiments were extended to 2,400 minutes because persulfate activation at this temperature is very slow.

4.2.3. Furfural analysis

Furfural concentration was measured using a UV/Vis spectrophotometer (Thermo Fisher Scientific, Model Evolution 600 Madison, WI 53711, US), as done in previous oxidation studies that degrade furfural [80-82]. The maximum wavelength for furfural was 258 nm. Calibration curves were made by using standards of known furfural concentrations and performing serial dilutions. Statistical analysis was performed using Microsoft Excel. Standard error (SE) of the data were represented by error bars in the figures and was calculated using Equation 4.1:

$$SE = \frac{s}{\sqrt{n}} \quad (4.1)$$

where s is the sample standard deviation and n is the number of observations.

4.2.4. "LEB10-X" and reaction byproduct analysis

Prior to analysis using gas chromatography mass spectrometry (GC/MS), samples were extracted using liquid-liquid extraction. The liquid-liquid extractions were performed with 3 mL of sample. The sample was pipetted into scintillation vials, 1 mL of hexane was added, the vials were vortexed for 30 seconds using a 115V Mini Vortex Mixer (Fisher Scientific, Pittsburgh, PA 15275, USA), and separated using a 6 mL polypropylene syringe (Fisher Scientific, Pittsburgh, PA 15275, USA). The hexane fraction was placed into a separate scintillation vial and the water fraction was placed back into the original scintillation vial. This was repeated three times, for a total of 3 mL hexane used per sample.

Spectra were obtained with a gas chromatograph (Agilent 7890B) equipped with a DB-1 capillary column (30 m x 0.25 mm inner diameter x 0.25 μ m film thickness) interfaced to a 5977A Mass Selective Detector (MSD) (Santa Clara, CA 95051, USA). The NIST08 mass spectral library database was used for substance analysis. Ultra-high purity helium purchased from Airgas Corporation was used as the carrier gas and maintained at 1.5 mL min⁻¹ (Knoxville, TN 37921,

USA). The GC was operated in splitless mode with an injection volume of 2 μL using a 10 μL syringe. The initial temperature of the GC was 40°C and was held for 2 minutes. The temperature ramp was 2.5°C/min to 100°C, which was held for 2 minutes. For samples with LEB-10X, the temperature ramp was extended to 200°C.

CHAPTER 5: Results and Discussion

5.1. GC/MS analysis of LEB-10X

The gas chromatogram displayed in Figure 1 shows the peak in the chromatogram identified as furfural and its mass spectrum. As mentioned previously, “LEB-10X” is used as an enzyme-breaking agent in hydraulic fracturing fluids. Enzyme breakers are added to hydraulic fracturing fluids to increase flowback. They are typically protein molecules that act as catalysts to break down the polymer gelling agents at specific sites. The approximate concentration of LEB-10X added to hydraulic fracturing fluids is 0.025 gallons per 1,000 gallons of water. Other compounds identified in LEB-10X were 5-hydroxymethylfurfural, 5-acetoxymethyl-2-furfuraldehyde, 1-methyl-1H-pyrazole-4-carboxaldehyde, 1-bromo-chloroethane, (E)-1,2-dichloroethylene, 2-fluoro-5-methoxypyrimidine (a cancer drug), chlorozotocin (used in cancer therapy), zearalenone (an estrogenic metabolite), and hemicellulosic compounds glucopyranose, galactapyranose, arbutin, and inositol.

5.2. Kinetic modeling and furfural persistence

Overall pseudo first-order rate coefficients by all potential oxidizing agents potentially produced ($S_2O_8^{2-}$, $SO_4^{\cdot -}$, HO^{\cdot} , etc.) for the loss of furfural were determined assuming irreversible first-order kinetics for all data. The overall pseudo first-order rate constant and half-life data obtained for all conditions is summarized in Tables 2 and 4. The overall rate constant for furfural degradation may be expressed as Equation 5.1:

$$\frac{C}{C_o} = k_{obs} * dt \quad (5.1)$$

where C is the furfural concentration expressed in mole per liter concentration at a specific time and k_{obs} is the overall pseudo first-order rate constant in s^{-1} .

In addition to the reaction rate constants for furfural degradation, these equations were also used to determine the persistence of furfural in water as shown in Figure 2. Persistence was assessed by calculating the furfural half-life using Equation 5.2:

$$t_{\frac{1}{2}} = \frac{\ln(2)}{k_{obs}} \quad (5.2)$$

where $t_{1/2}$ is the furfural half-life in seconds. The abiotic hydrolysis half-life of furfural in water at

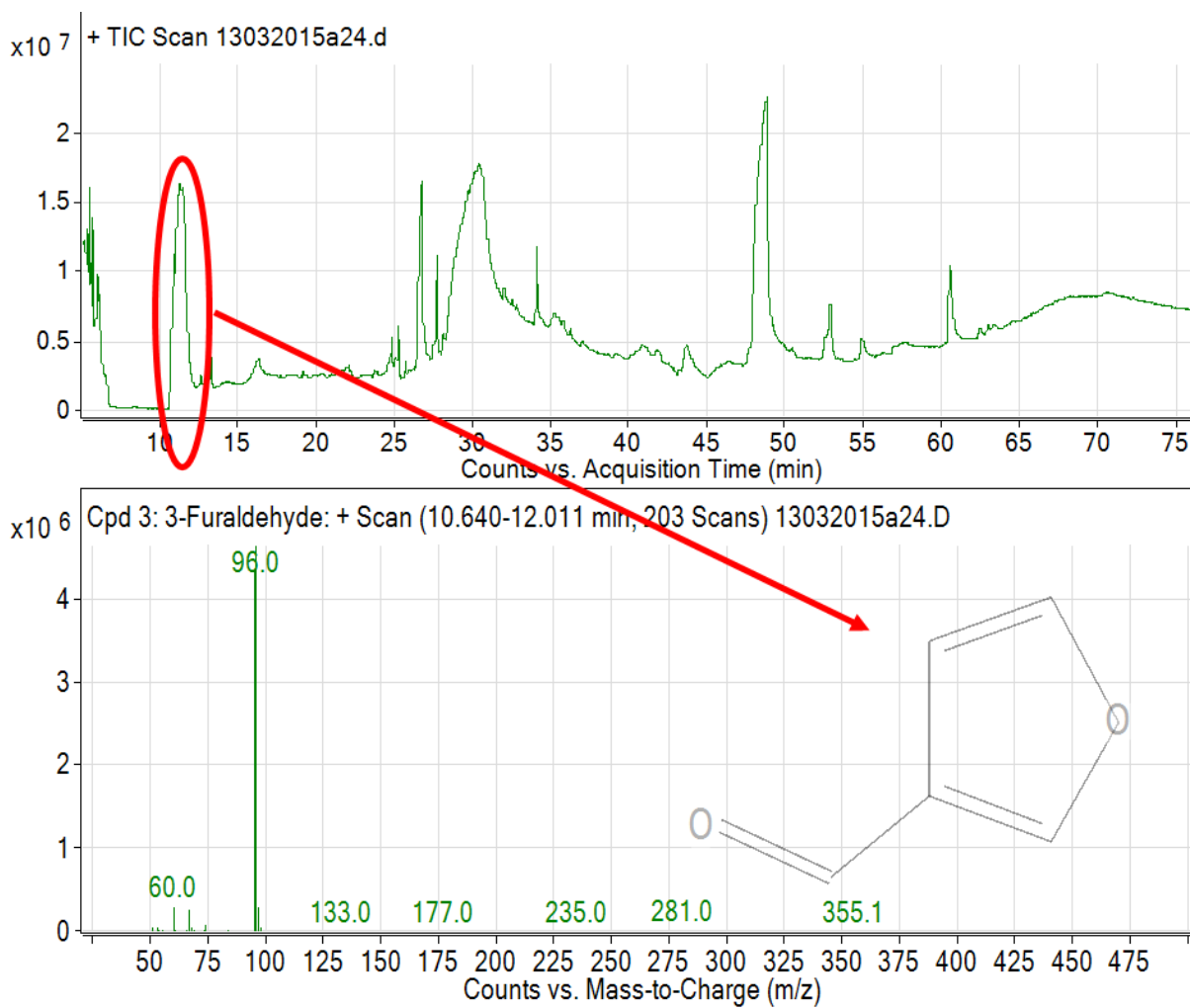


Figure 1. Gas chromatogram and mass spectrum of LEB-10X.

pH 5.4 when no persulfate is present was determined to be $84.7 \text{ days} \pm 0.34$ signifying that furfural is persistent in water. When hydraulic fracturing brine without iron at pH 2.54 was introduced, the furfural half-life increased to $188 \text{ days} \pm 7.19$. The half-life of furfural in brine with 23.33 mg L^{-1} of ferric sulfate at pH 2.54 was determined to be $199 \text{ days} \pm 7.67$. The increased persistence of furfural in this environment suggests that the presence of inorganic salts and acidic conditions found in hydraulic fracturing fluids may increase the persistence of the certain organic constituents [83-85]. The use of sodium persulfate as a means for remediating groundwater could be very effective in destroying persistent furfural contamination.

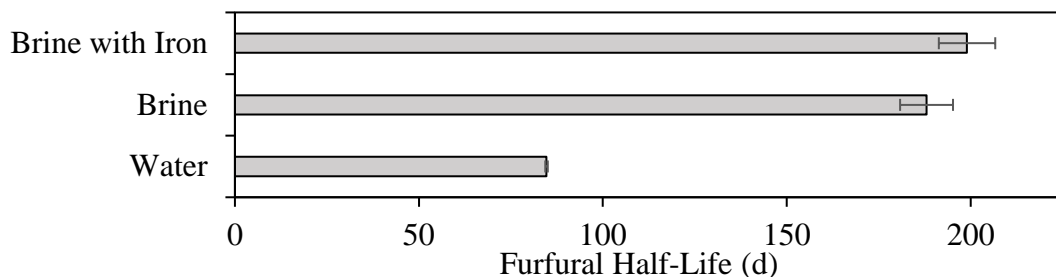


Figure 2. Half-life of furfural in water, hydraulic fracturing brine, and hydraulic fracturing brine with 23.33 mg L^{-1} ferric sulfate (no sodium persulfate added).

5.3. Furfural oxidation via sodium persulfate in water

5.3.1. Temperature effects

Furfural ($C_i = 120 \text{ mg L}^{-1}$, 1.25 mM) oxidation with 21 mM sodium persulfate increased as temperature increased from 20 to 60°C (pH initial = 5.4). Figure 3a shows the decrease in furfural concentration from 30 to 60°C with no ferric sulfate present, while Figure 3b displays the decrease in furfural concentration with 23.33 mg L^{-1} ferric sulfate. As seen in these figures, minimal furfural degradation occurred at 30 and 40°C , suggesting that the persulfate anion is not responsible for furfural oxidation. Rather, the sulfate radical is responsible for furfural removal once adequate temperatures are achieved to activate the persulfate. In both cases, furfural oxidation by thermally activated sodium persulfate followed pseudo-first order rate models. The resulting values of k_{obs} are given in Table 2.

As seen in Figure 4 , an Arrhenius model was used to determine the activation energy (E_a) of furfural oxidation with and without the presence of ferric sulfate at pH 2.54 and 5.4. Activation Energy was calculated using Equation 5.3:

$$\ln k_{obs} = \ln A - \frac{E_a}{RT} \quad (5.3)$$

where A is the frequency factor in s^{-1} , R is the universal gas constant in $J K^{-1} mol^{-1}$, and T is absolute temperature in Kelvin. For furfural oxidation by thermally activated 21 mM sodium persulfate at pH 5.4, the activation energy was determined to be $107.3 \text{ kJ mol}^{-1}$ ($R^2 = 0.97$). In the presence of 23.33 mg L^{-1} ferric sulfate at pH 5.4, the activation energy of furfural oxidation was $107.6 \text{ kJ mol}^{-1}$ ($R^2=0.99$). At a lower pH of 2.54, the activation energy was determined to be 74.3 kJ mol^{-1} ($R^2 = 0.99$) without ferric sulfate and 75.2 kJ mol^{-1} ($R^2 = 0.99$) with ferric sulfate. Due to difference in activation energy, this suggests that, in the presence of an organic contaminant, low pH is a stronger catalyst than Fe (III) for furfural oxidation via persulfate because it significantly lowers the energy barrier by inducing a different reaction pathway [86, 87]. The addition of Fe (III) also induces a different reaction pathway; however, the frequency of reaction collisions varies depending on the pseudo-first order reaction rate constant. Consider Equation 4.3 in the form of Equation 5.4.

$$k_{obs} = Ae^{\frac{-E_a}{RT}} \quad (5.4)$$

When two different reactions with the same activation energy are considered, the remaining variables in this equation are shown in Equation 5.5.

$$\frac{k_{obs,1}}{A_1} = \frac{k_{obs,2}}{A_2} \quad (5.5)$$

For reactions with ferric sulfate in solution, higher pseudo-first order reaction rate constants are observed. For these higher reaction rate constants, a larger frequency factor will also be observed, which is the case for these reactions as shown in Table 3. The frequency factor is independent of temperature and relies on the frequency of furfural to radical collisions and on a steric factor – the relative orientation of molecules during collision [88]. The reaction rate constants are proportional to the frequency factors. In the presence of Fe (III), the frequency of radical-to-furfural collisions increases, but it is proportional to the pseudo-first order rate constant; thus, the activation energy remains constant.

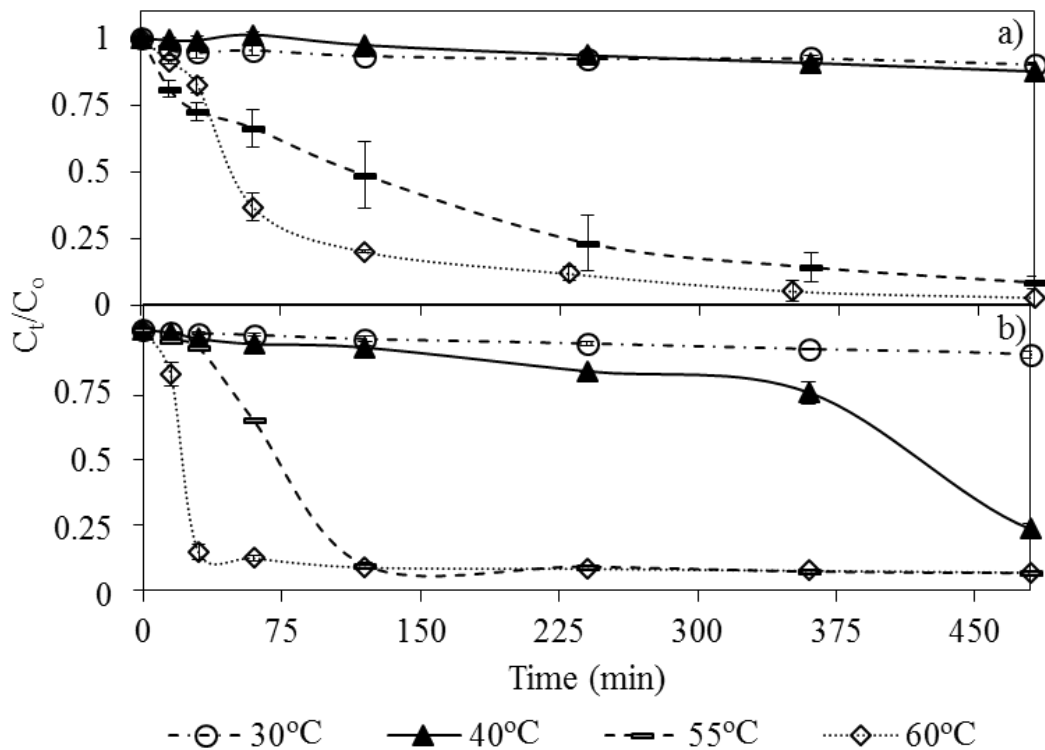


Figure 3. The decrease in furfural concentration over the course of 480 minutes with (a) 0 mg L⁻¹ (b) 23.33 mg L⁻¹ ferric sulfate. The initial pH was 5.4 and the initial dose of sodium persulfate was 21 mM.

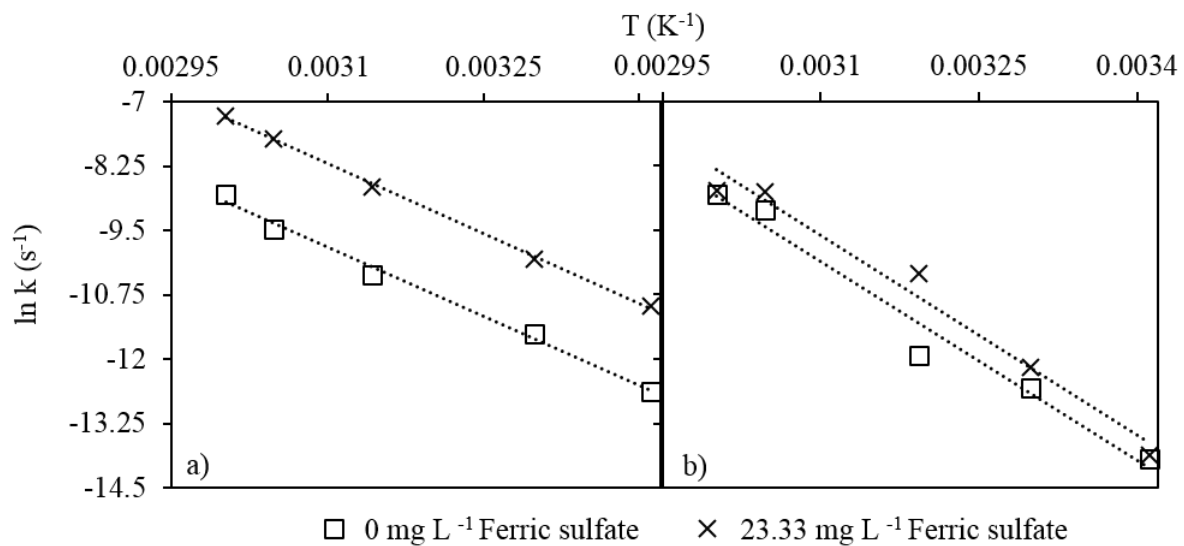


Figure 4. Arrhenius plots for the oxidation of furfural by sodium persulfate with 0 and 23.33 mg L⁻¹ ferric sulfate with an pH of a) 2.54 and b) 5.4.

Table 2. Pseudo first-order reaction rate constants for furfural oxidation via activated persulfate.

[Na ₂ S ₂ O ₈] _i (mM)	[Fe ₂ (SO ₄) ₃] _i (mg L ⁻¹)	pH	T (°C)	k _{obs} (s ⁻¹)	t _{1/2} (d)	R ²
Varying temperature						
21	0	5.4	20	8.79x10 ⁻⁷	9.13	0.95
21	0	5.4	30	3.53x10 ⁻⁶	2.27	0.91
21	0	5.4	40	6.53x10 ⁻⁶	1.23	0.93
21	0	5.4	55	9.12x10 ⁻⁵	0.0879	0.98
21	0	5.4	60	1.49x10 ⁻⁴	0.0542	0.94
21	23.33	5.4	20	9.46x10 ⁻⁷	8.48	0.93
21	23.33	5.4	30	5.20x10 ⁻⁶	1.54	0.97
21	23.33	5.4	40	1.24x10 ⁻⁵	0.647	0.96
21	23.33	5.4	55	1.59x10 ⁻⁴	0.0504	0.91
21	23.33	5.4	60	1.62x10 ⁻⁴	0.0496	0.93
21	0	2.54	20	3.29x10 ⁻⁶	2.44	0.96
21	0	2.54	30	1.02x10 ⁻⁵	0.788	0.92
21	0	2.54	45	1.53x10 ⁻⁵	0.525	0.89
21	0	2.54	55	9.64x10 ⁻⁵	0.0864	0.96
21	0	2.54	60	1.52x10 ⁻⁴	0.0528	0.95
21	23.33	2.54	20	1.18x10 ⁻⁵	0.679	0.91
21	23.33	2.54	30	4.28x10 ⁻⁵	0.187	0.89
21	23.33	2.54	45	1.70x10 ⁻⁴	0.473	0.95
21	23.33	2.54	55	4.47x10 ⁻⁴	0.0179	0.93
21	23.33	2.54	60	6.89x10 ⁻⁴	0.0116	0.98
Varying pH						
5	0	2.54	55	7.26x10 ⁻⁵	0.110	0.97
5	0	5.4	55	1.58x10 ⁻⁵	0.508	0.97
5	0	10.4	55	4.95x10 ⁻⁵	0.162	0.95
10	0	2.54	55	8.87x10 ⁻⁵	0.0904	0.94
10	0	5.4	55	3.69x10 ⁻⁵	0.218	0.98

Table 2. Continued.

[Na ₂ S ₂ O ₈] _i (mM)	[Fe ₂ (SO ₄) ₃] _i (mg L ⁻¹)	pH	T (°C)	k _{obs} (s ⁻¹)	t _{1/2} (d)	R ²
10	0	10.4	55	4.92x10 ⁻⁵	0.163	0.95
15	0	2.54	55	9.18x10 ⁻⁵	0.0874	0.95
15	0	5.4	55	6.67x10 ⁻⁵	0.120	0.97
15	0	10.4	55	9.07x10 ⁻⁵	0.0883	0.98
5	23.33	2.54	55	3.21x10 ⁻⁴	0.0250	0.95
5	23.33	5.4	55	8.21x10 ⁻⁵	0.0979	0.98
10	23.33	2.54	55	3.93x10 ⁻⁴	0.0204	0.94
10	23.33	5.4	55	1.44x10 ⁻⁴	0.0558	0.94
15	23.33	2.54	55	4.11x10 ⁻⁴	0.0195	0.96
15	23.33	5.4	55	1.52x10 ⁻⁴	0.0529	0.96
Varying persulfate dose						
0.6	0	5.4	55	5.24x10 ⁻⁶	1.53	0.98
5	0	5.4	55	1.58x10 ⁻⁵	0.508	0.97
10	0	5.4	55	3.96x10 ⁻⁵	0.203	0.98
15	0	5.4	55	6.67x10 ⁻⁵	0.120	0.97
21	0	5.4	55	9.12x10 ⁻⁵	0.0879	0.98
0.6	23.33	5.4	55	2.01x10 ⁻⁵	0.399	0.95
5	23.33	5.4	55	8.21x10 ⁻⁵	0.0977	0.98
10	23.33	5.4	55	1.44x10 ⁻⁴	0.0557	0.94
15	23.33	5.4	55	1.52x10 ⁻⁴	0.0528	0.96
21	23.33	5.4	55	1.59x10 ⁻⁴	0.0505	0.91
Varying ferric sulfate concentration						
15	5	5.4	55	1.30x10 ⁻⁴	0.0617	0.93
15	10	5.4	55	1.56x10 ⁻⁴	0.0514	0.95
15	25	5.4	55	1.64x10 ⁻⁴	0.0489	0.99
15	50	5.4	55	1.40 x10 ⁻⁴	0.0573	0.99
15	100	5.4	55	8.42x10 ⁻⁵	0.0953	0.95

Table 3. Arrhenius parameters for furfural removal.

[Fe ₂ (SO ₄) ₃] _i (mg L ⁻¹)	pH	E _a (kJ mol ⁻¹)	A (s ⁻¹)	R ²
0	5.4	107.3	9.52 x 10 ¹²	0.97
23.33	5.4	107.6	1.83 x 10 ¹³	0.99
0	2.54	74.3	5.78 x 10 ⁷	0.99
23.33	2.54	75.2	4.07 x 10 ⁸	0.99

5.3.2. Effect of pH

As observed in Figure 4, the activation energy is significantly impacted by the solution pH. Therefore, the effect of pH (2.54, 5.4, 10.4) on furfural degradation with and without the presence of ferric sulfate for three different sodium persulfate concentrations (5, 10, 15 mmol L⁻¹) was further investigated. The decrease in furfural concentration over time for each pH and sodium persulfate dose is shown in the Appendix Figure A 3, a through f. Figure 5 displays the effect of pH on the pseudo first-order rate constant without the presence of ferric sulfate when the persulfate dose is 5, 10, and 15 mM. Whether iron was present or not, at all persulfate concentrations, the highest degradation rate constant was achieved when the pH tested was 2.54. Elevated pH (10.4), also known as alkaline activation [49], was only tested without ferric sulfate in solution. In basic conditions, the rate constant was higher than in neutral pHs, but not as high as the acidic conditions. This suggests that low pHs are preferable for the oxidation of furfural using heat activated sodium persulfate [46, 89].

At both acidic and neutral pHs, Reaction 2.1 occurs in oxidation using heat activated sodium persulfate. At acidic pHs, sulfate radical rate production is increased due to additional breakdown of the persulfate anion as shown in Reactions 5.1 and 5.2 [90, 91]. The increased production of radicals raises the probability for radical-to-contaminant reactions and causes the higher observed pseudo first-order reaction rate constant for furfural removal.



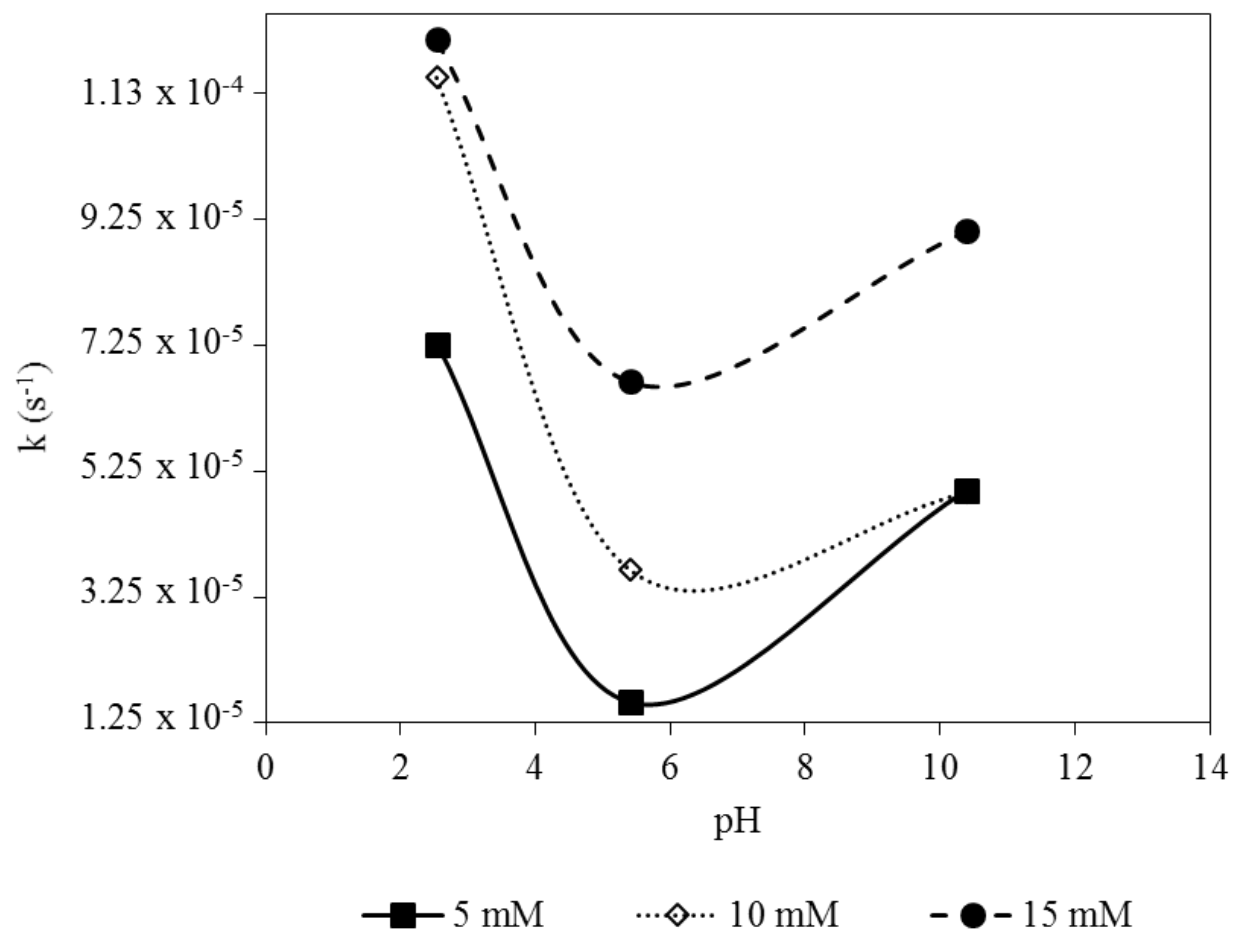


Figure 5. Influence of pH on the reaction rate constant of furfural degradation with 0 mg L^{-1} ferric sulfate and at 55°C .

At basic pH, the sulfate radicals form less selective hydroxyl radicals, as shown in Reaction 5.3 [50, 65]. The production of the hydroxyl radical may decrease contaminant removal efficiency because very fast radical-to-radical reactions may be favored over radical-to-contaminant interactions [54, 89]. When this occurs, the persulfate source is depleted without removing furfural. The radical-to-radical reactions cause the observed pseudo first-order reaction rate constants to be lower than those observed in acidic conditions.



5.3.3. Effect of initial persulfate dose

Five persulfate doses were tested, 0.6, 5, 10, 15, and 21 mM, at 55°C and pH of 5.4. The decrease in furfural concentration over time is shown in Figure 6. With 23.33 mg L⁻¹ ferric sulfate, more than 90% removal was achieved after 120 minutes with initial sodium persulfate doses of 10, 15, and 21 mM. Without the addition of ferric sulfate, the greatest removal, 97%, was not obtained until 480 minutes of reacting with a persulfate dose of 21 mM. Figure 7 displays the effect of persulfate doses on the observed pseudo first-order rate constant with both 0 and 23.33 mg L⁻¹ ferric sulfate. In both cases, the relationship between initial persulfate concentration and the pseudo first order rate constant is linear ($R^2 = 0.99$ for the solution without ferric sulfate, $R^2 = 0.96$ for solutions with 23.33 mgL⁻¹ ferric sulfate). Higher initial persulfate concentrations led to higher furfural degradation rates.

5.3.4. Effect of iron concentration

The effect of ferric sulfate concentration on furfural degradation with an initial persulfate dose of 15 mM may be seen in Figure 8. The greatest amount of furfural removal (95%) was achieved when the concentration of ferric sulfate was 5, 10 and 25 mg L⁻¹ within 480 minutes. When 25 mg L⁻¹ ferric sulfate was in solution, 95% removal was achieved within 160 minutes, whereas 10 mg L⁻¹ ferric sulfate took 250 minutes and 5 mg L⁻¹ ferric sulfate took the whole 480 minutes to achieve the same removal. The overall furfural removal achieved with 50 and 100 mg L⁻¹ ferric sulfate was 88 and 80%, respectively. Figure 9 displays the effect of ferric sulfate concentration on the pseudo first order reaction rate constant. The highest observed rate constant was determined to be 1.65×10^{-4} with 25 mg L⁻¹ ferric sulfate in solution. The rate constant gradually increases until the ferric sulfate concentration reached 25 mg L⁻¹ ferric sulfate.

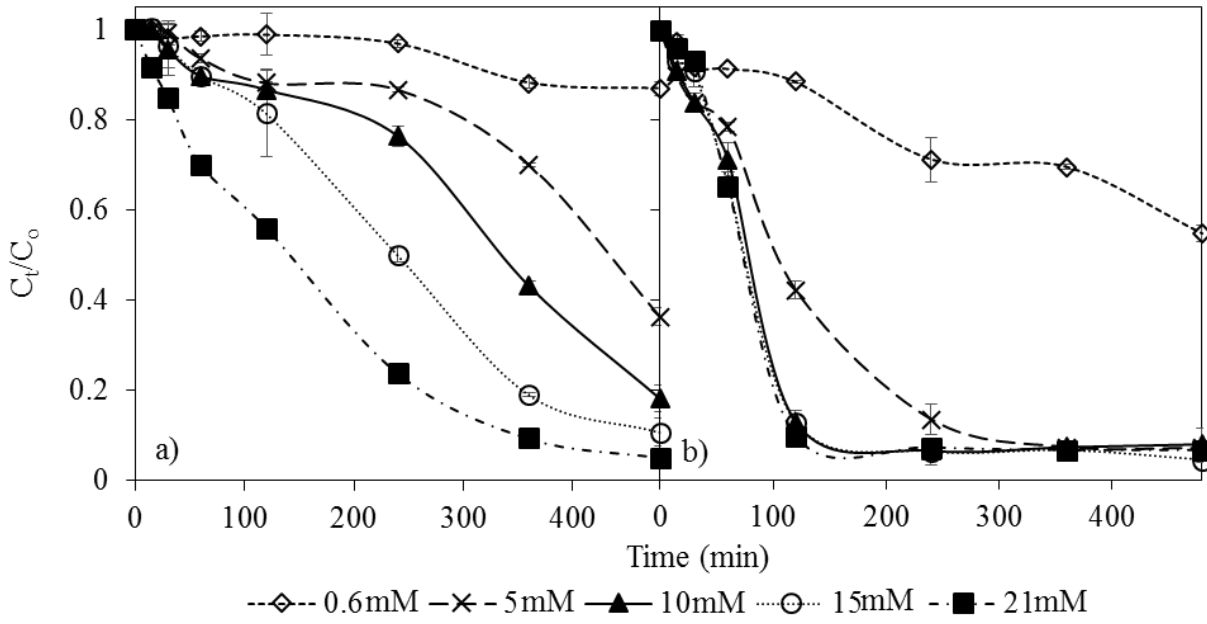


Figure 6. Effect of persulfate dose on the concentration of furfural at 55°C at pH 5.4 with (a) 0 mg L⁻¹ ferric sulfate and (b) 23.33 mg L⁻¹ ferric sulfate.

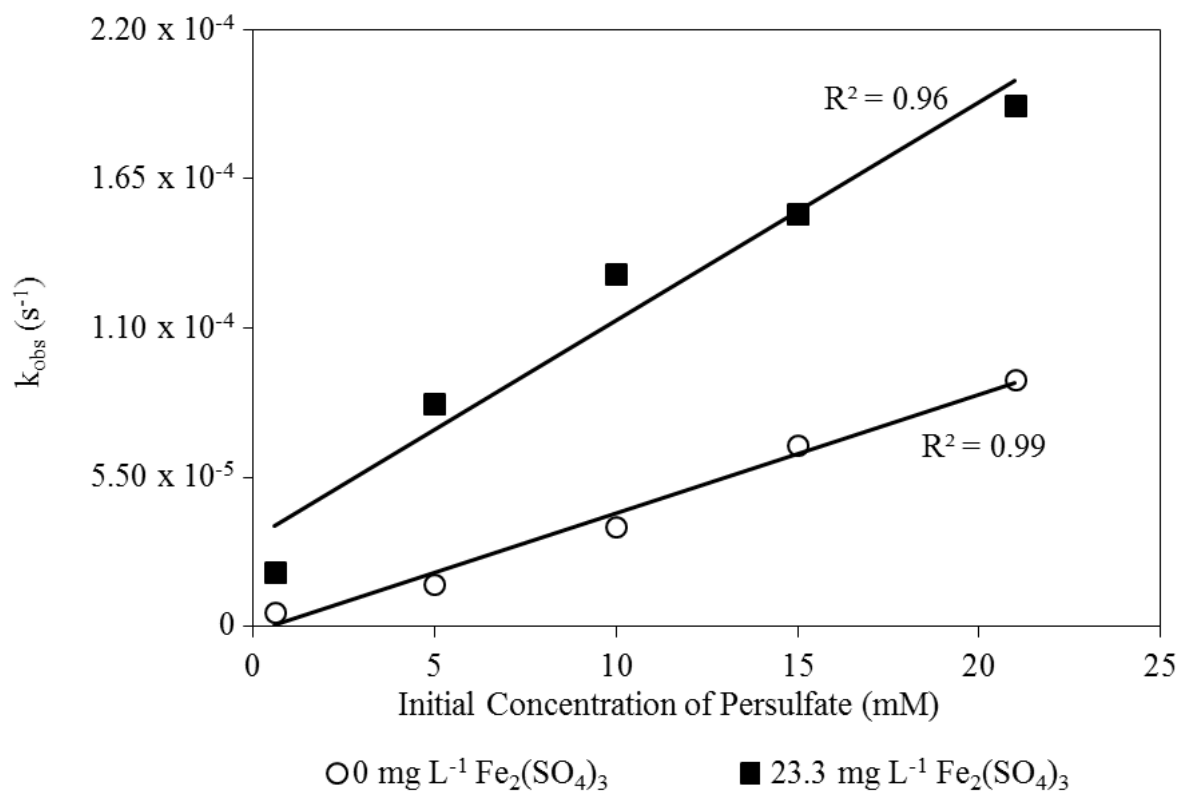


Figure 7. Relationship between the initial concentration of persulfate and the reaction rate constant at 55°C and pH 5.4 with 0 and 23.33 mg L⁻¹ ferric sulfate.

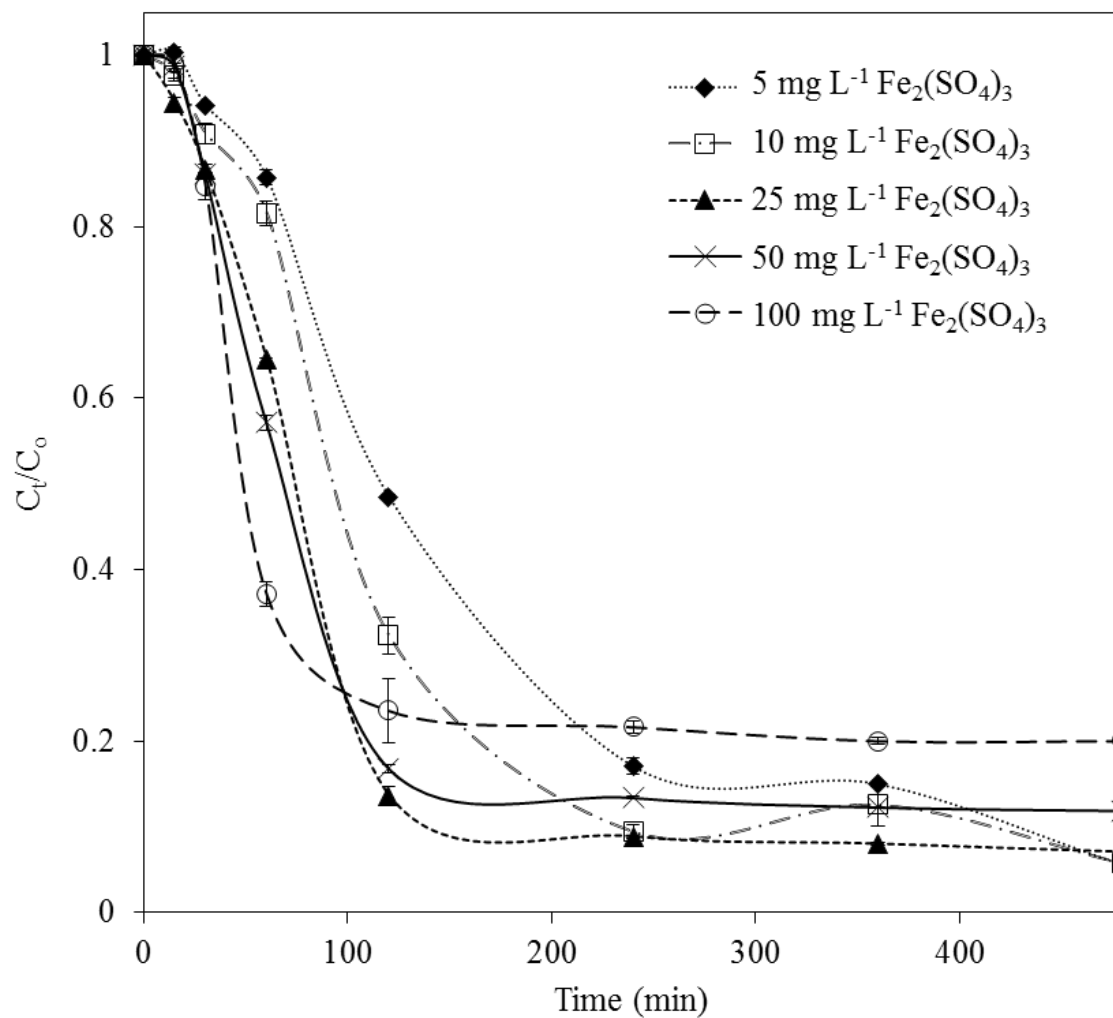


Figure 8. Effect of iron concentration on furfural degradation over time at 55°C, pH 5.4, and initial persulfate dose of 15 mM.

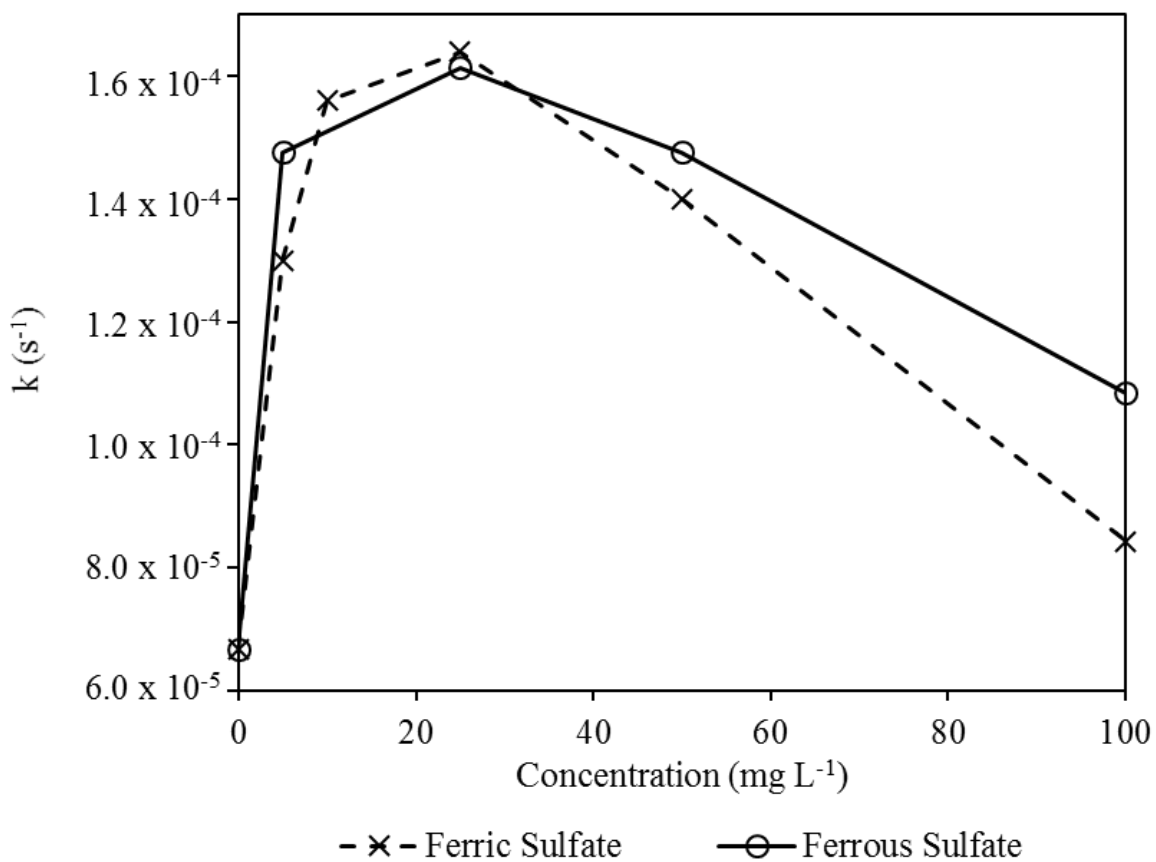


Figure 9. Comparison of the use of Fe(III) and Fe(II) to activate persulfate for furfural removal (pH 5.4, T = 55°C, initial persulfate dose = 15 mM).

At ferric sulfate concentrations greater than 25 mg L^{-1} , the pseudo first order reaction rate constant begins to decrease. This indicates that there is a maximum iron dose that may be used for ISCO of furfural for every persulfate dose. When the initial persulfate dose is 15 mM and the ferric sulfate concentrations was greater than 25 mg L^{-1} , the reaction between $\text{SO}_4^{\cdot-}$ and excess iron may consume $\text{SO}_4^{\cdot-}$ faster than $\text{SO}_4^{\cdot-}$ can react with furfural [92].

The effect of ferric sulfate versus ferrous sulfate (FeSO_4) dosing on furfural degradation is also displayed in Figure 9. As shown, whether the iron was Fe (II) or Fe (III) has very little effect on the pseudo-first order reaction rate constant. The maximum iron sulfate dose remains at 25 mg L^{-1} . At the highest concentration of Fe (II), 100 mg L^{-1} , 80% furfural removal was achieved within 15 minutes, but only 84% total removal was achieved after 480 minutes. This suggests that Fe (II) was in excess and most of the persulfate was activated within the first 15 minutes. For 5 and 50 mg L^{-1} Fe (II), the overall furfural removal (86%) was achieved after 120 and 30 minutes of reacting, respectively. The greatest furfural removal was 90% and was achieved using a Fe (II) dose of 25 mg L^{-1} after 60 minutes. For both Fe (II) and Fe (III), the optimal concentration was 25 mg L^{-1} . The results show that using Fe (II) or Fe (III) for furfural degradation by activated persulfate has little effect on the reaction rate constant, which agrees with the findings of Rodriguez *et al* [87].

5.3.5. Byproduct identification and pathway discussion

The reaction pathway was investigated using GC/MS to identify the reaction by-products of furfural oxidation via persulfate. Generally, free radicals attack the nearest stable molecule and generate a radical intermediate or another reaction byproduct. The degradation pathway for furfural oxidation is suggested as shown in Figure 10 based on the reaction by-products identified in samples taken at different time points in the experiment. The detection of 2-methylbutanoic acid and ethyl-3-furoate after 5 minutes occurred prior to the detection of 3-furancarboxylic acid at 15 minutes. After 15 minutes, 3-furancarboxylic acid was detected for the remainder of the experiment. 2-methylbutanoic acid and ethyl-3-furoate were detected until 30 minutes and were not detected any time after this point.

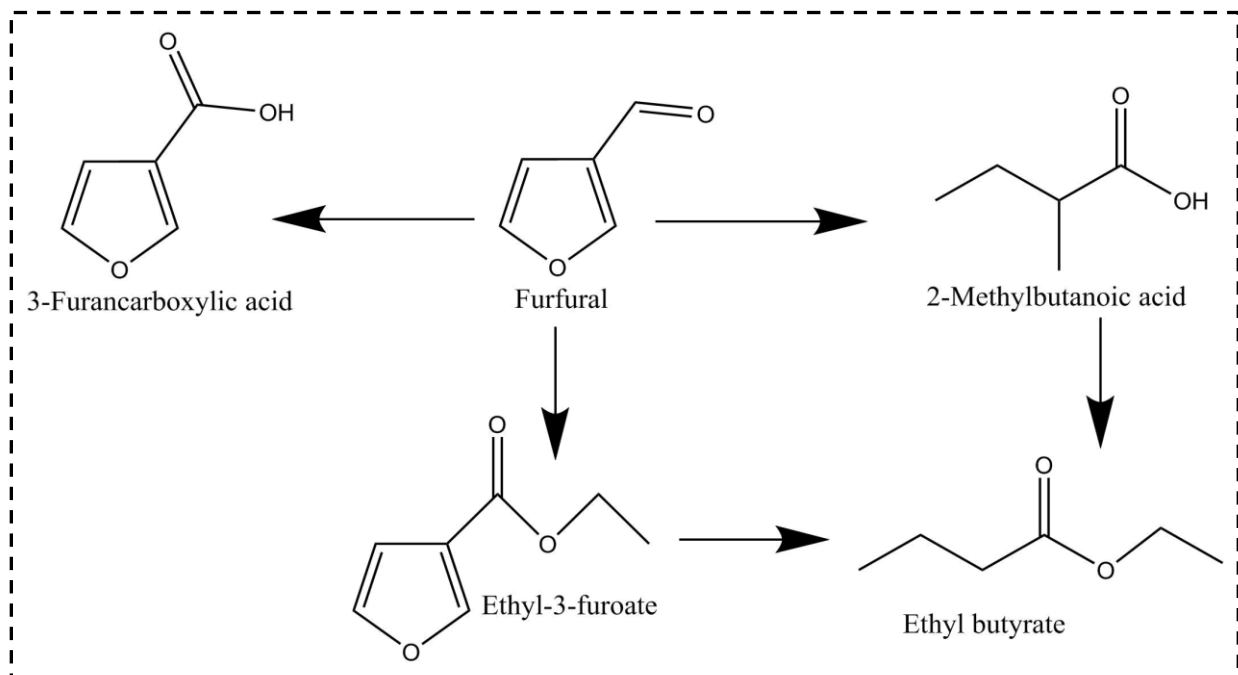


Figure 10. Proposed reaction pathway.

When radicals attack furfural, the electron dense locations, the aromatic ring and the aldehyde functional group, are targeted. Upon attack of electron dense oxygen atom on the aromatic ring, 2-methylbutanoic acid is produced via ring opening. Upon the attack of the aldehyde functional group, ethyl-3-furoate and 3-furancarboxylic acid are produced. The slightly acidic reaction conditions are suitable for the oxidation of the aldehyde group into a carboxylic acid. It is most likely that furfural first transforms into the hydrate form and is subsequently attacked very rapidly by the persulfate oxidizing agent to form 3-furancarboxylic acid.

These initial byproducts are also susceptible to further oxidation. Ethyl butyrate formation is likely due to the radical attack of both ethyl-3-furoate and 2-methylbutanoic acid. Ester formation can occur when a carboxylic acid is in the presence of an alcohol and an acid. While no alcohols were detected using GC/MS, it is possible that ethanol may be present in solution as a reaction byproduct allowing for the formation of ethyl butyrate.

5.4. Furfural degradation via sodium persulfate in hydraulic fracturing conditions

5.4.1. Effect of temperature and Arrhenius model

Pseudo first-order reaction rate constants for all batch experiments performed in hydraulic fracturing brine are displayed in Table 4. Figure 11 displays the effect of temperature on furfural degradation in the presence of hydraulic fracturing brine (pH 2.54, 21 mM initial sodium persulfate dose). Figure 11a shows the decrease in furfural concentration over time in acidic hydraulic fracturing brine when no iron is present at different temperatures, while Figure 11b shows the same conditions, but contains 23.33 mg L⁻¹ of ferric sulfate. With or without ferric sulfate, as temperature increases, greater furfural removal is achieved in a shorter amount of time. Without ferric sulfate at 60°C in hydraulic fracturing brine (pH 2.54), 97% furfural removal is not achieved until 480 minutes of reacting. In non-hydraulic fracturing conditions without ferric sulfate (pH 2.54, 60°C), the overall removal, 98%, was achieved after 360 minutes. When ferric sulfate is present in hydraulic fracturing conditions, 97% furfural removal is achieved after 120 minutes at 60°C (pH 2.54). In non-hydraulic fracturing conditions at the same pH, temperature, and iron concentration, 94% furfural removal was achieved after 120 minutes. Anions, including chloride, nitrate, and bicarbonate, have been shown to have an impact on contaminant removal by persulfate

Table 4. Pseudo first-order reaction rate constant of furfural degradation in the presence of hydraulic fracturing brine.

$[\text{Na}_2\text{S}_2\text{O}_8]_i$ (mM)	$[\text{Fe}_2(\text{SO}_4)_3]_i$ (mg L ⁻¹)	pH	T (°C)	k_{obs} (s ⁻¹)	$t_{1/2}$ (d)	R^2
Varying temperature						
21	0	2.54	20	1.19×10^{-6}	6.74	0.95
21	0	2.54	30	3.27×10^{-6}	2.45	0.90
21	0	2.54	40	9.96×10^{-6}	0.806	0.95
21	0	2.54	55	1.11×10^{-4}	0.0723	0.99
21	0	2.54	60	1.80×10^{-4}	0.0446	0.98
21	23.33	2.54	20	2.69×10^{-6}	2.98	0.96
21	23.33	2.54	30	1.97×10^{-5}	0.407	0.93
21	23.33	2.54	40	4.14×10^{-5}	0.194	0.98
21	23.33	2.54	55	3.68×10^{-4}	0.0218	0.92
21	23.33	2.54	60	5.20×10^{-4}	0.0154	0.95
Varying pH						
5	23.33	2.54	55	8.87×10^{-5}	0.0904	0.96
5	23.33	5.4	55	5.72×10^{-5}	0.140	0.93
10	23.33	2.54	55	1.76×10^{-4}	0.0456	0.95
10	23.33	5.4	55	6.89×10^{-5}	0.116	0.97
15	23.33	2.54	55	2.68×10^{-4}	0.0299	0.98
15	23.33	5.4	55	1.05×10^{-4}	0.0764	0.97
Varying persulfate dose						
0.6	0	2.54	55	8.40×10^{-6}	0.955	0.92
5	0	2.54	55	3.33×10^{-5}	0.241	0.99
10	0	2.54	55	7.05×10^{-5}	0.114	0.94
15	0	2.54	55	7.59×10^{-5}	0.106	0.95
21	0	2.54	55	1.11×10^{-4}	0.0723	0.99
0.6	23.33	2.54	55	7.60×10^{-6}	1.06	0.92
5	23.33	2.54	55	8.87×10^{-5}	0.0904	0.96
10	23.33	2.54	55	1.76×10^{-4}	0.0456	0.95
15	23.33	2.54	55	2.68×10^{-4}	0.0299	0.98
21	23.33	2.54	55	3.68×10^{-4}	0.0218	0.92

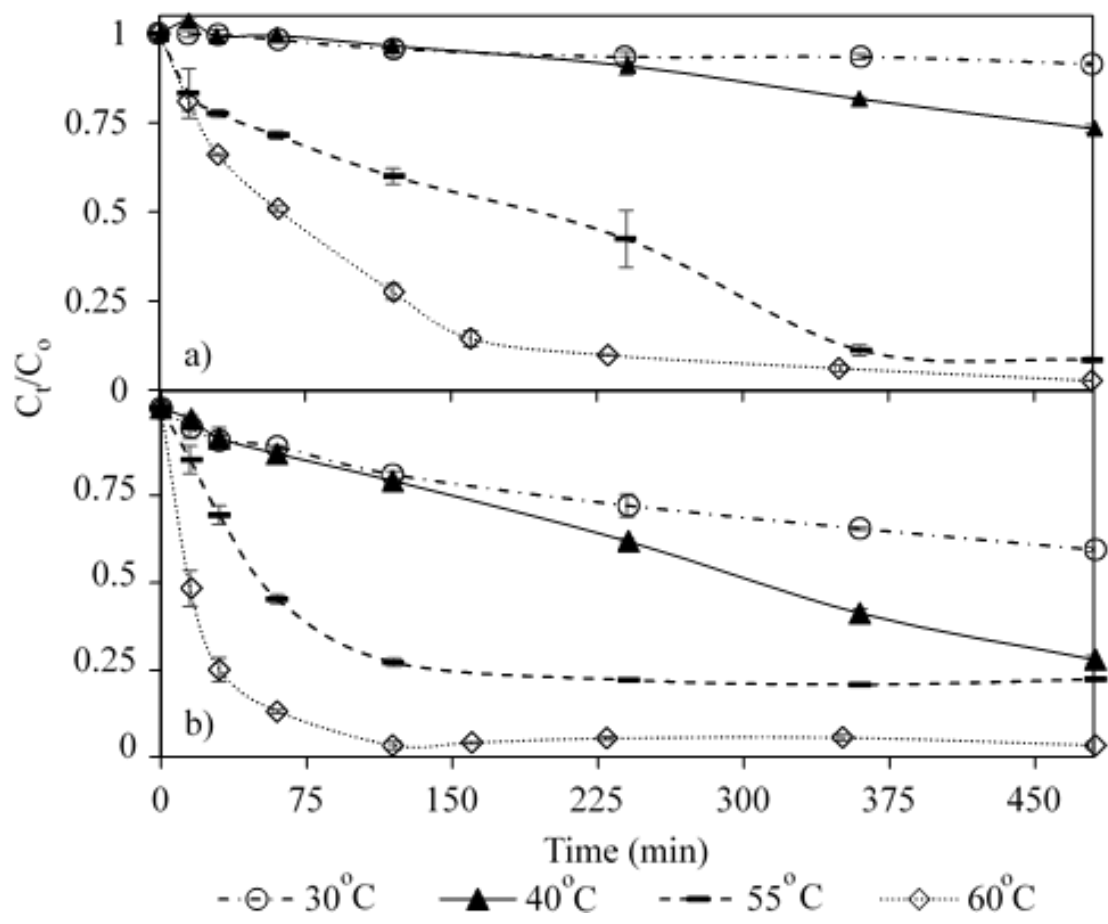


Figure 11. The effect of temperature on furfural degradation in the presence of hydraulic fracturing brine. Experimental conditions: pH 2.54, 21 mM dose of sodium persulfate, and a) 0 mg L⁻¹ ferric sulfate and b) 23.33 mg L⁻¹ ferric sulfate.

oxidation by scavenging the radicals in solution [93, 94]. The presence of hydraulic fracturing brine had little impact on the degree of furfural removal at pH 2.54 compared to the impact it has on the time it took to achieve maximum removal.

Activation energy for furfural degradation in the presence of 0 and 23.33 mg L⁻¹ ferric sulfate was determined with an initial sodium persulfate dose of 21 mM (pH = 2.54). As seen in Figure 12, activation energy was determined using the Arrhenius model. For experiments with 0 mg L⁻¹ ferric sulfate, the activation energy in hydraulic fracturing brine was determined to be 105.6 kJ mol⁻¹ (R²=0.99). With 23.33 mg L⁻¹ ferric sulfate, the activation energy was determined to be 105.1 kJ mol⁻¹ (R²=0.99). While very different pseudo-first-order reaction rate constants and furfural removals were achieved for the solutions with and without iron, the activation energy was not affected. As discussed earlier, the presence of iron does impact that frequency at which furfural molecules comes into contact with radical molecules. However, this frequency is proportional to the pseudo-first order reaction rate constant and does not change the activation energy of furfural removal. Reactions with iron have higher pseudo-first order reaction rate constants and thus, higher frequency factor values as shown in Table 5. Therefore, Fe (III) does not follow the true definition of acting as a catalyst for furfural removal even in the presence of hydraulic fracturing brine.

Table 5. Arrhenius parameters in the presence of hydraulic fracturing brine.

[Fe ₂ (SO ₄) ₃] _i (mg L ⁻¹)	pH	E _a (kJ mol ⁻¹)	A (s ⁻¹)	R ²
0	2.54	105.6	5.99 x 10 ¹²	0.99
23.33	2.54	105.1	1.77 x 10 ¹³	0.99

5.4.2. Effect of brine pH

Figure 13 displays the change in persulfate concentration over time at different pHs (55°C). Figure 13a displays the changes in concentration at pH 5.4 and Figure 13b displays the changes at pH 2.54. At low pHs, furfural degradation via sodium persulfate is much less affected by persulfate dose than at neutral pH. As seen in Figure 13b, at pH 2.54, maximum furfural

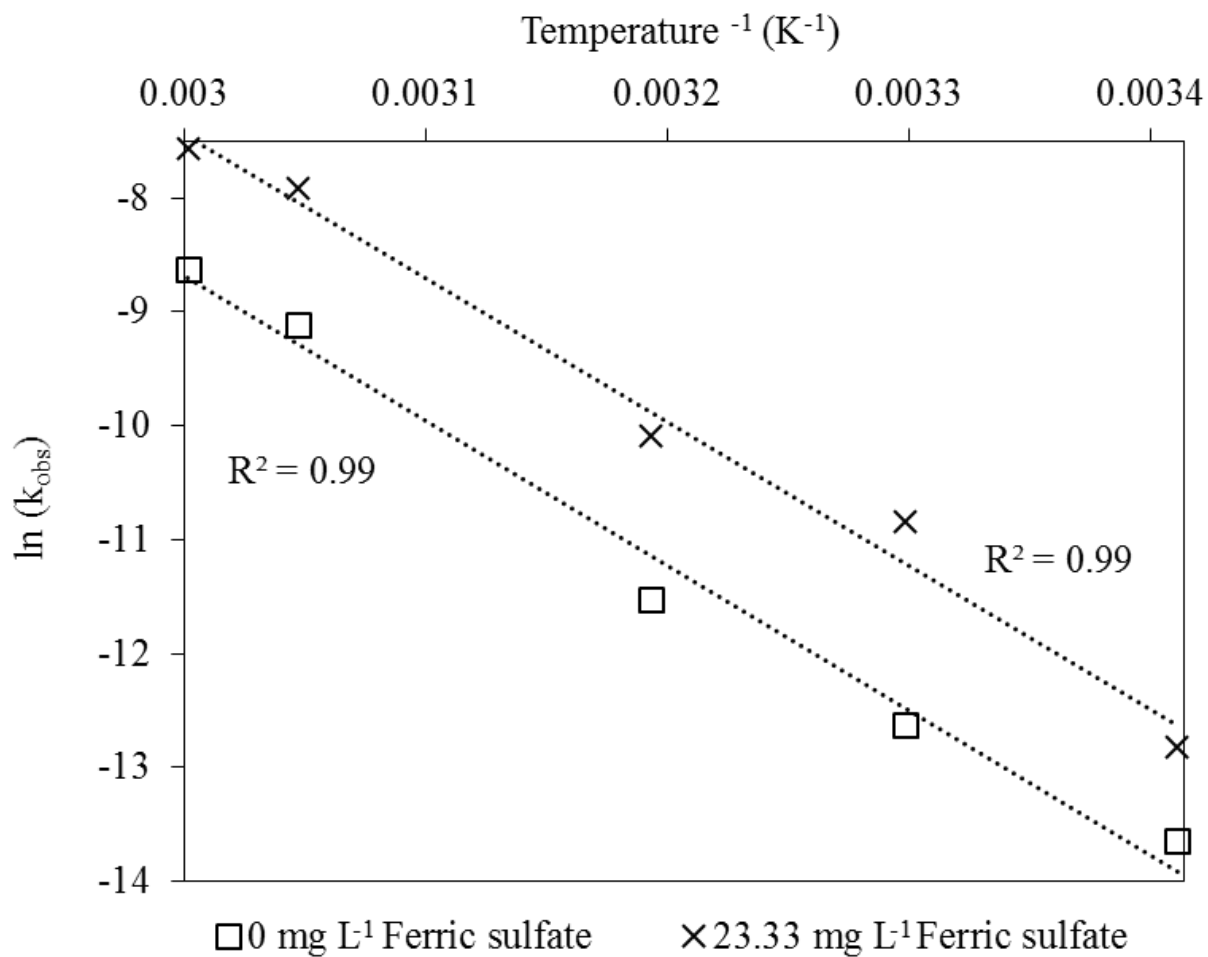


Figure 12. Arrhenius plot of furfural degradation in the presence of hydraulic fracturing brine with and without ferric sulfate (pH 2.54, initial sodium persulfate dose of 21 mM).

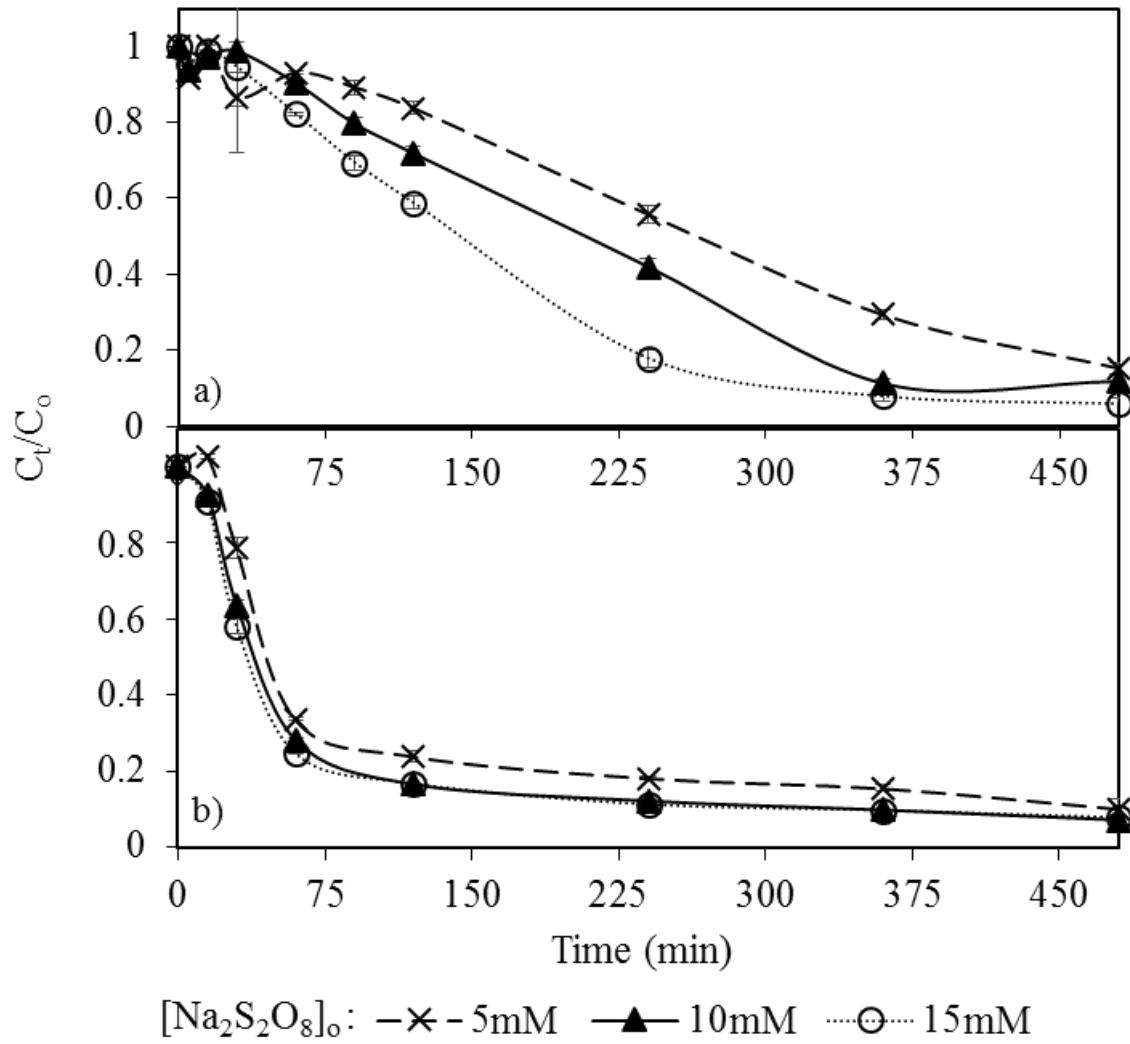


Figure 13 . Effect of initial pH – a) 5.4, b) 2.54 – of the hydraulic fracturing brine at different doses of sodium persulfate (55°C).

removal (93%) is achieved after 480 minutes of reacting with 5, 10, and 15 mM sodium persulfate. By 120 minutes, 84% removal is already achieved with sodium persulfate doses of 10 and 15 mM while 75% furfural removal is achieved with 5 mM sodium persulfate. At pH 5.4, maximum removal achieved at 480 minutes by sodium persulfate doses of 5, 10, 15 mM are 85, 89, and 95%, respectively. Furfural removal occurs more gradually at pH 5.4 than at pH 2.54. At 120 minutes of reacting, 10, 21, and 32% of furfural has been removed with 5, 10, and 15 mM sodium persulfate, respectively.

5.4.3. Effect of initial persulfate dose

Figure 14 displays the five doses of persulfate, 0.6, 5, 10, 15, and 21 mM, which were tested at 55°C and pH of 2.54. Figure 14a displays the furfural removal over time with 0 mg L⁻¹ ferric sulfate and Figure 14b displays the removal with 23.33 mg L⁻¹ ferric sulfate. Without ferric sulfate, more furfural removal is achieved with higher doses of sodium persulfate in shorter time periods. After 480 minutes of reacting, the higher doses of sodium persulfate, 10, 15, and 21 mM, 95% furfural removal is achieved. With 23.33 mg L⁻¹ ferric sulfate, the difference between furfural removal with 5, 10, 15, and 21 mM doses of sodium persulfate is less distinct. However, the pseudo first-order reaction rate constant increases very linearly with the persulfate dose ($R^2=1.00$) as seen in Figure 14c. Reactions without ferric sulfate also follow this linear trend ($R^2=0.97$). Despite the presence of hydraulic fracturing brine, higher doses of persulfate led to higher pseudo first-order reaction rate constants.

5.4.4. Overall impact of hydraulic fracturing brine on kinetics

The presence of ions, especially chloride and bicarbonate, in solution has been shown to have a quenching effect on contaminant removal in heat-activated persulfate. However, the degree of scavenging by ions is highly dependent on the temperature at which the reaction is performed [89, 90, 95]. Higher temperatures, such as 100 °C, have a lower tolerance for ion presence than lower temperatures, such as 20°C [89]. Figure 15 displays the difference in furfural removal at pH 2.54 between water and hydraulic fracturing brine at 30, 45, 55, and 60°C. Figure 15 a and b are in water with 0 and 23.33 mg L⁻¹ ferric sulfate, respectively. Figure 15 c and d are in hydraulic fracturing brine with 0 23.33 mg L⁻¹ ferric sulfate, respectively. It is observed that hydraulic

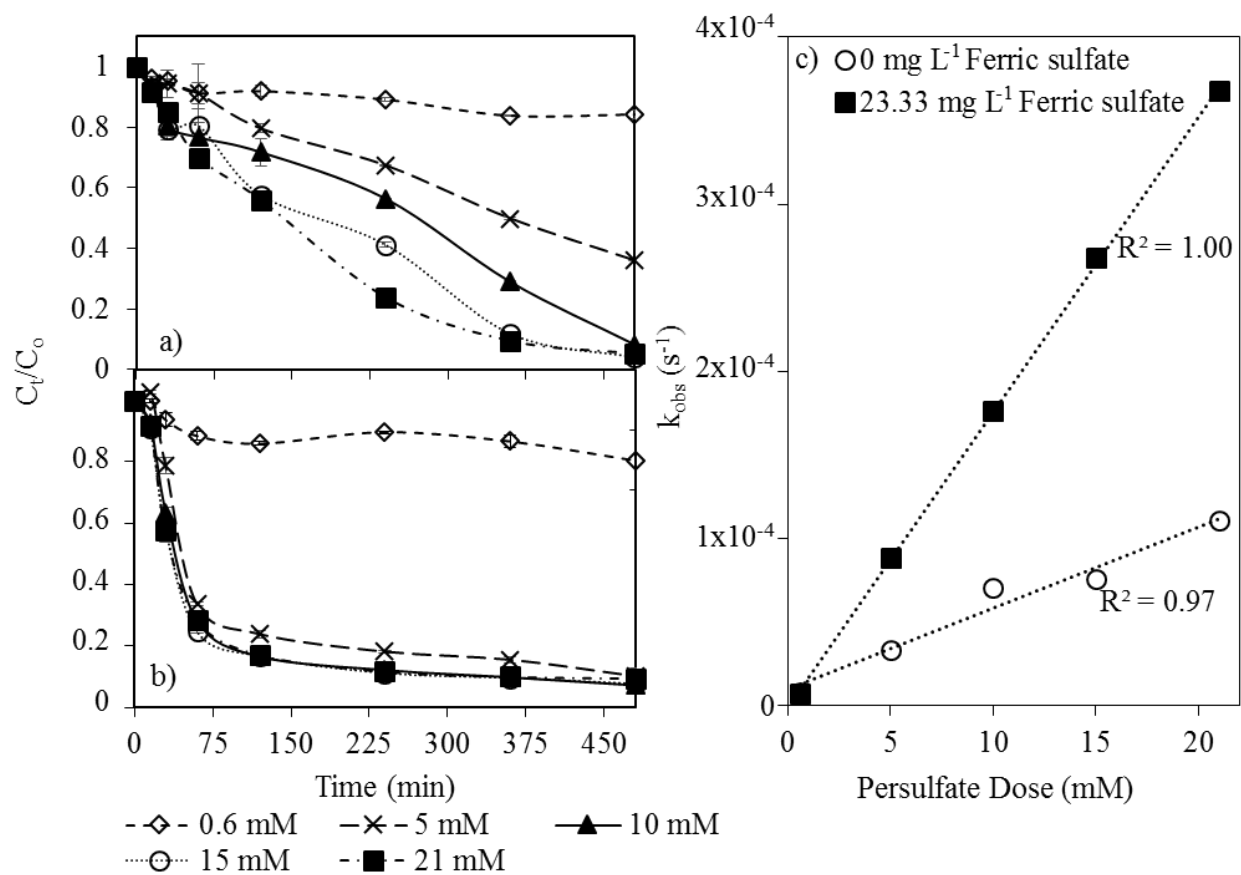


Figure 14. The initial dose of persulfate has an effect on furfural removal with a) 0 mg L⁻¹ ferric sulfate and b) 23.33 mg L⁻¹ ferric sulfate. The effect of persulfate dose on pseudo-first order reaction rate constant is shown in c) with and without ferric sulfate.

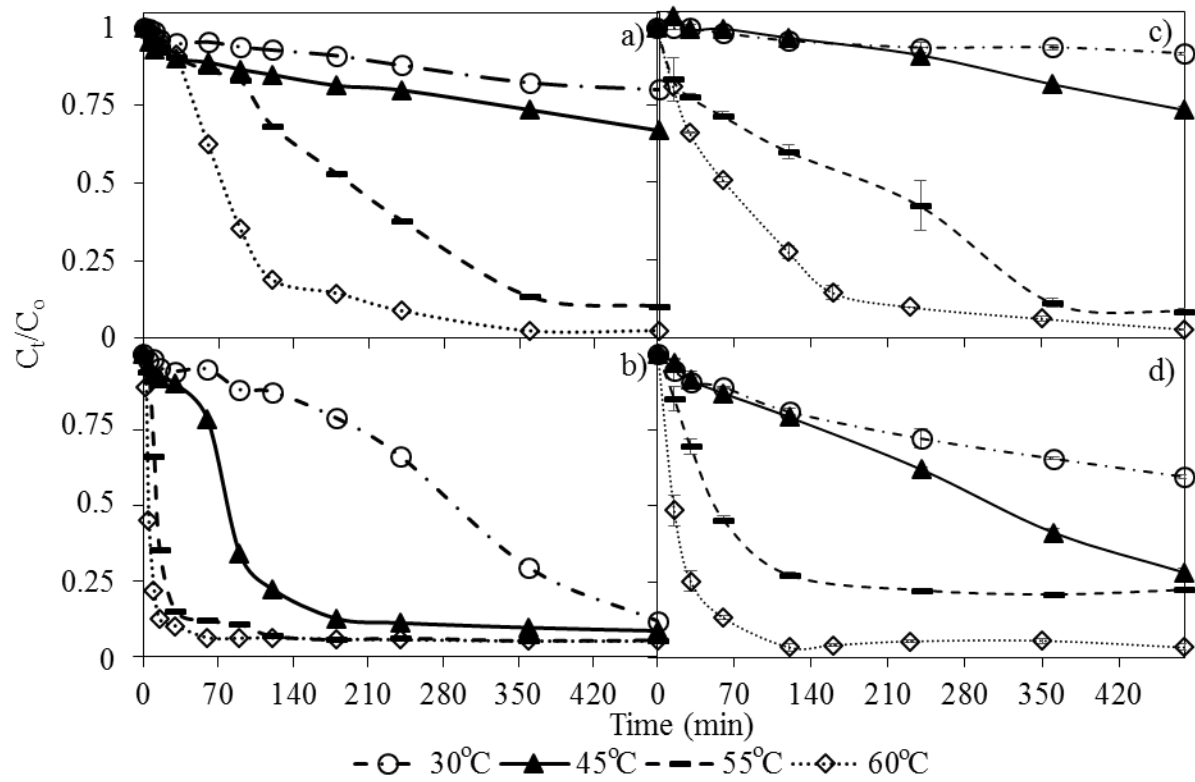


Figure 15. Furfural removal (pH 2.54) in water and a) 0 and b) 23.33 mg L⁻¹ ferric sulfate and in hydraulic fracturing brine with c) 0 and d) 23.33 mg L⁻¹ ferric sulfate at different temperatures.

fracturing brine does have a quenching effect on furfural removal at both the higher and lower temperatures tested in this study. The quenching effect on contaminant removal by hydraulic fracturing brine is most noticeable in the solutions that contain ferric sulfate. The ferric sulfate activates persulfate very rapidly, which encourages radical-to-radical and radical-to-anion interactions to occur in place of some of the radical-to-furfural interactions.

The radical-to-anion interactions also have an impact on the pseudo-first order reaction rate constant at pH 2.54 and 5.4 and initial sodium persulfate doses of 5, 10, and 15 mM as seen in Figure 16 (55°C, 23.33 mg L⁻¹ ferric sulfate). At lower pH, the difference between the pseudo first-order reaction rate constants at all sodium persulfate doses are more pronounced than at neutral pH. Again, this is likely due to the increase in persulfate activation as discussed in section 4.3.2. and, therefore, an increase in radical-to-radical or radical-to-anion interactions.

Figure 15 displays how the activation energy of furfural degradation via persulfate in hydraulic fracturing brine compares to the activation energy of furfural degradation in water. The activation energy in water with a pH of 5.4 and the activation energy in hydraulic fracturing brine with a pH of 2.54 are within 2.5% of each other. In acidic water, the activation energy is 30 kJ mol⁻¹ less than the other two. This suggests that solution pH and hydraulic fracturing ions impact the minimum energy that must be available for the chemical reaction between furfural and the generated radicals to occur. In Figure 17, the impact of the presence of iron on activation energy may also be observed. As discussed earlier, the presence of ferric sulfate does impact the observed pseudo first-order reaction rate. However, the presence of ferric sulfate has little influence on the activation energy. This suggests that lower pH, rather than the addition of ferric sulfate, is a more effective catalyst for the oxidation of furfural via persulfate by providing an alternative route for the reaction with lower activation energy.

5.4.5. Byproduct identification in hydraulic fracturing brine

Furfural oxidation via sodium persulfate in the presence of furfural brine produced the same reaction byproducts as presented earlier without brine. Compounds produced in the absence of hydraulic fracturing brine were observed in experiments conducted in the brine. In hydraulic fracturing brine, 2-methylbutanoic acid, ethyl furoate, and 3-furancarboxylic acid were detected within the first 5 minutes of the reaction. Figure 18 displays the reaction pathway and the additional

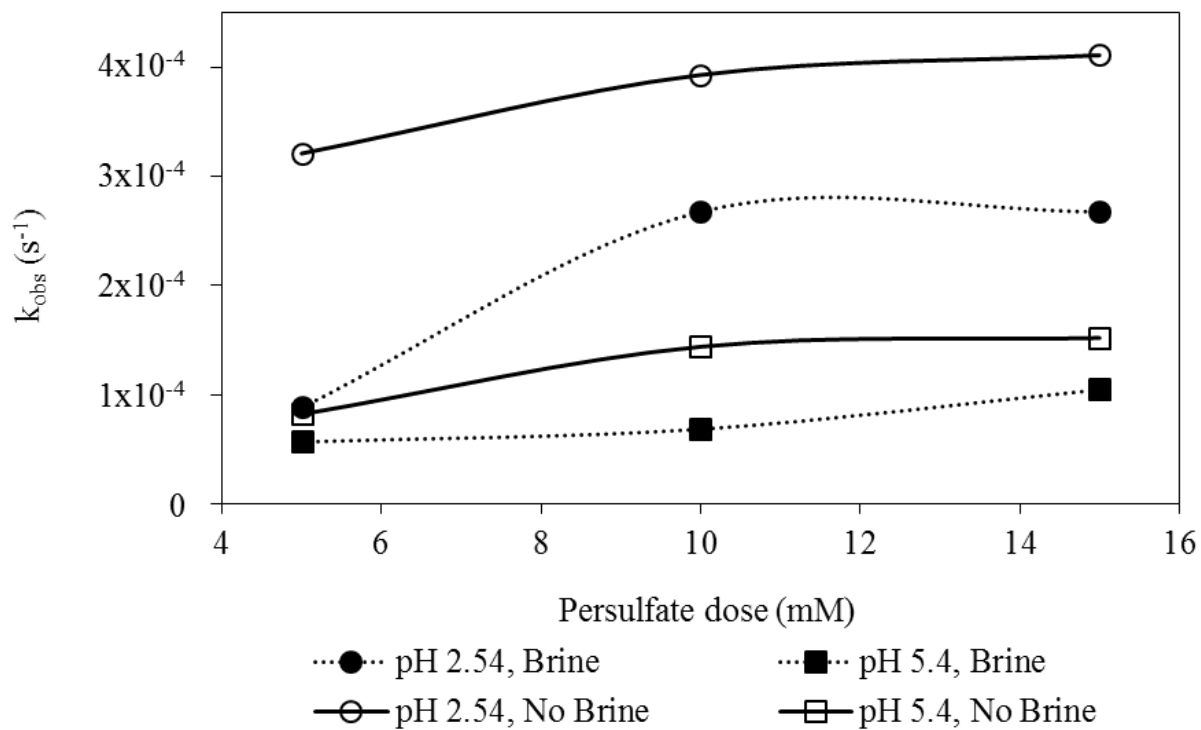


Figure 16. Effect of having brine in solution on the pseudo first-order reaction rate constant (55°C , 23.33 mg L^{-1} ferric sulfate).

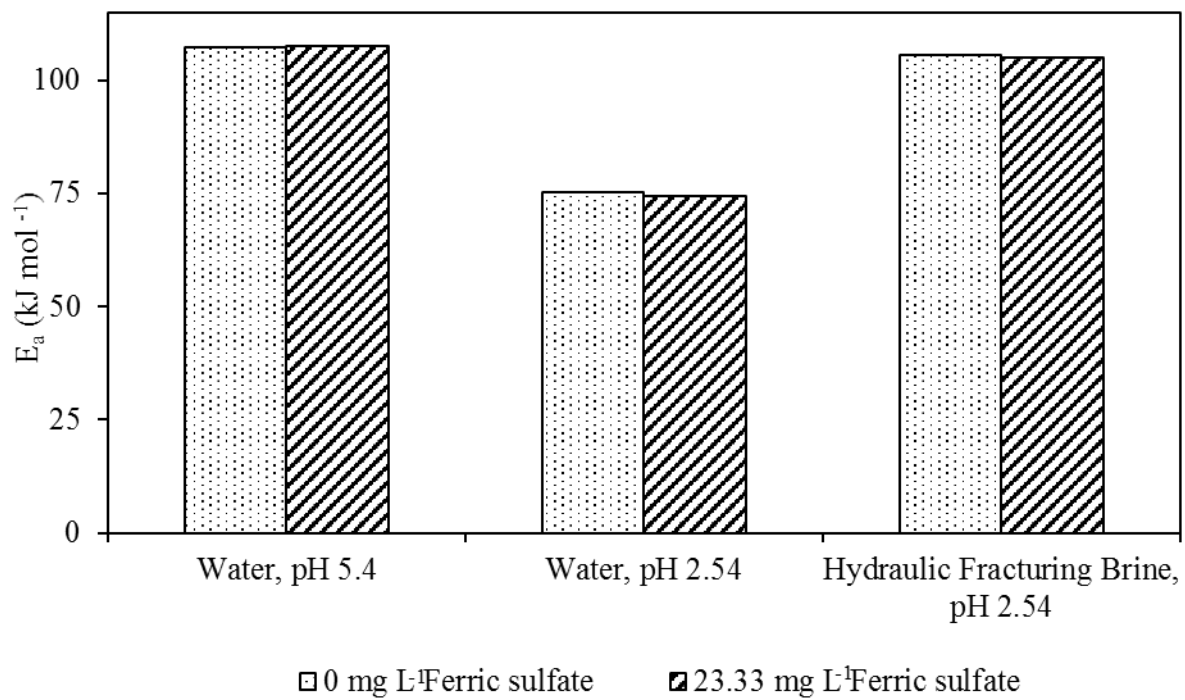


Figure 17. Comparison of all established activation energies.

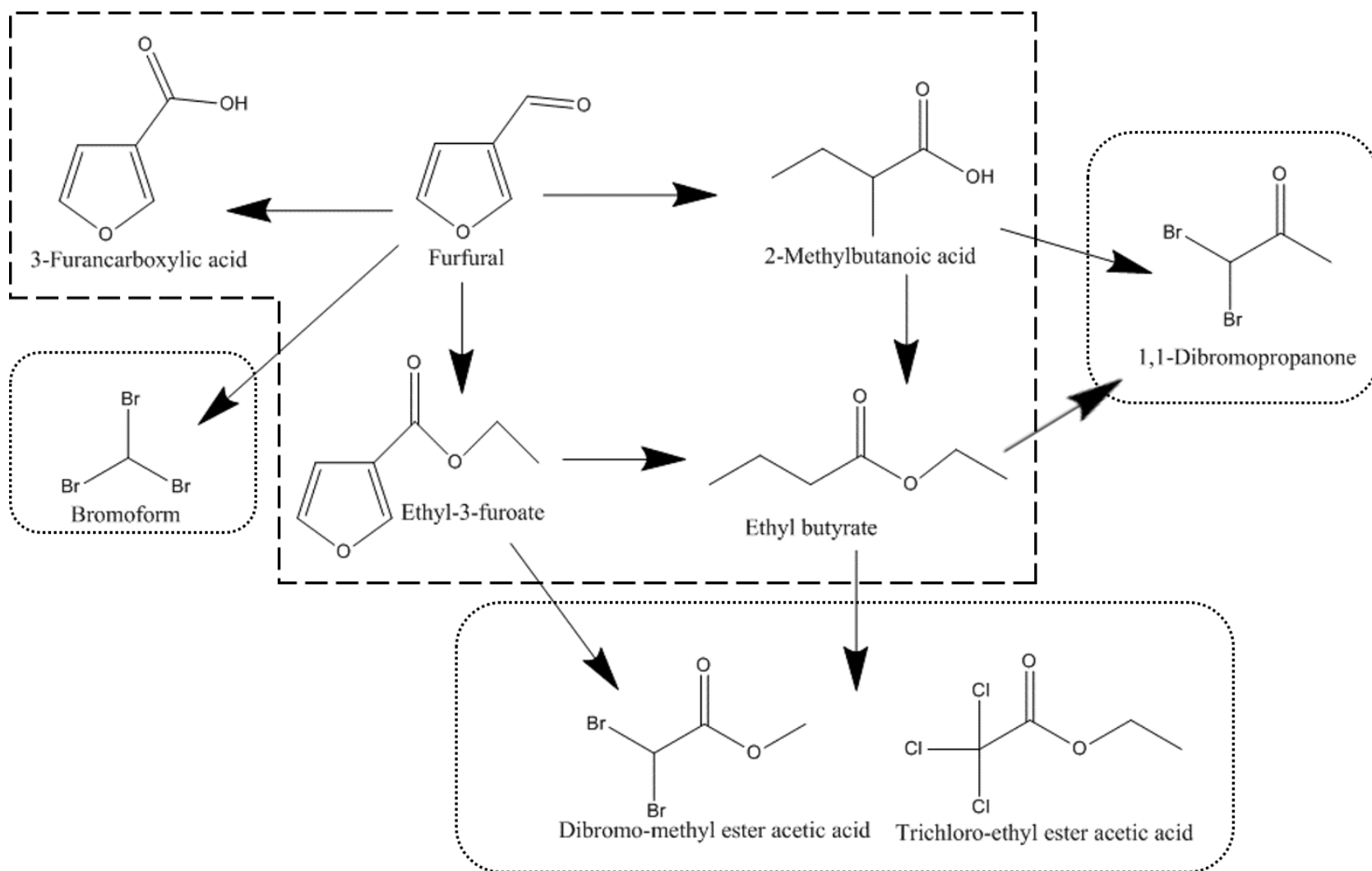


Figure 18. Reaction byproducts of furfural oxidation in the presence of hydraulic fracturing brine.

compounds produced in the presence of hydraulic fracturing brine. Bromoform was detected as early on as five minutes and persisted throughout the remainder of experiment. Bromoform was verified with a standard and the mass spectrum of the standard compared to the mass spectrum of the bromoform detected in the 480-minute sample may be found in the Appendix, Figure A 4. Additional halogenated compounds detected and their time of appearance were dibromo-methyl ester acetic acid at 240 minutes, 1,1-dibromopropanone at 480 minutes, and trichloro-ethyl ester acetic acid at 480 minutes.

The halogenated compounds detected are DBPs. Their formation stems from rapid radical-to-halogen interaction with subsequent attack on furfural or any one of the furfural degradation byproducts. Bromoform is a THM that has been regulated in the US since 1979 [96]. The current drinking water standard for total THMs is 0.08 mg L^{-1} [97]. 1,1-dibromopropanone is a haloketone (HK), which are not currently regulated by the US EPA. This may be attributable to the lack of toxicity data on HKs - they have been shown to cause oxidative stress in human cells, but have not been studied enough to be classified as carcinogens [96, 98]. Dibromo-methyl ester acetic acid and trichloro-ethyl ester acetic acid have similar structures to HAAs. Due to the high pH of hydraulic fracturing brine and the probability of alcohols present in solution from furfural oxidation, esterification may occur as explained earlier with ethyl butyrate. This suggest that it is likely that the HAAs parent compound are also present in solution, but not detected using GC/MS. Current methods used to detect HAAs require sample derivatization using acidic conditions and liquid-liquid extraction with methyl tertiary butyl ether or pentane, which are similar to extraction conditions used in this study [99]. However, it is unclear whether these compounds are byproducts of furfural oxidation or derivatization from the extraction method. Of these DBPs, bromoform is the only one to have been detected in hydraulic fracturing produced fluids [100].

5.6. Furfural degradation at elevated pressure

Experiments were conducted at without pressure applied (14.7 psi) and with 3,000 psi pressure applied because persulfate is continuously added to the reactor so that the concentration within the reactor was 5 mM. Furfural removal in hydraulic fracturing brine (pH 2.54) over time is displayed in the Appendix in Figure A 5 without pressure applied and in Figure A 6 with 3,000 psi applied at different temperatures. The reaction rate constants were calculated for each

temperature and tested. Using these rate constants, activation energies were calculated and plotted based on the Arrhenius model as shown in Figure 19. In experiments performed in the reactor with no pressure applied, the activation energy was $150.15 \text{ kJ mol}^{-1}$ ($R^2=0.97$). With 3,000 psi applied to the reactor, activation energy was 81.7 kJ mol^{-1} ($R^2= 0.96$). The activation energy difference suggest that a pressure increase can act as catalyst for contaminant removal via activated persulfate. While theoretical studies have been performed to simulate the kinetics of high pressure atmospheric OH-initated oxidation, this is the first experimental work to investigate the impact of pressure on ISCO. Reaction byproducts in the high pressure experiments were examined and the same compounds were detected in the batch experiments. One additional compound, a halgoentated keto acid, 3,3-dimethyl-5-bromo-levulinic acid was detected.

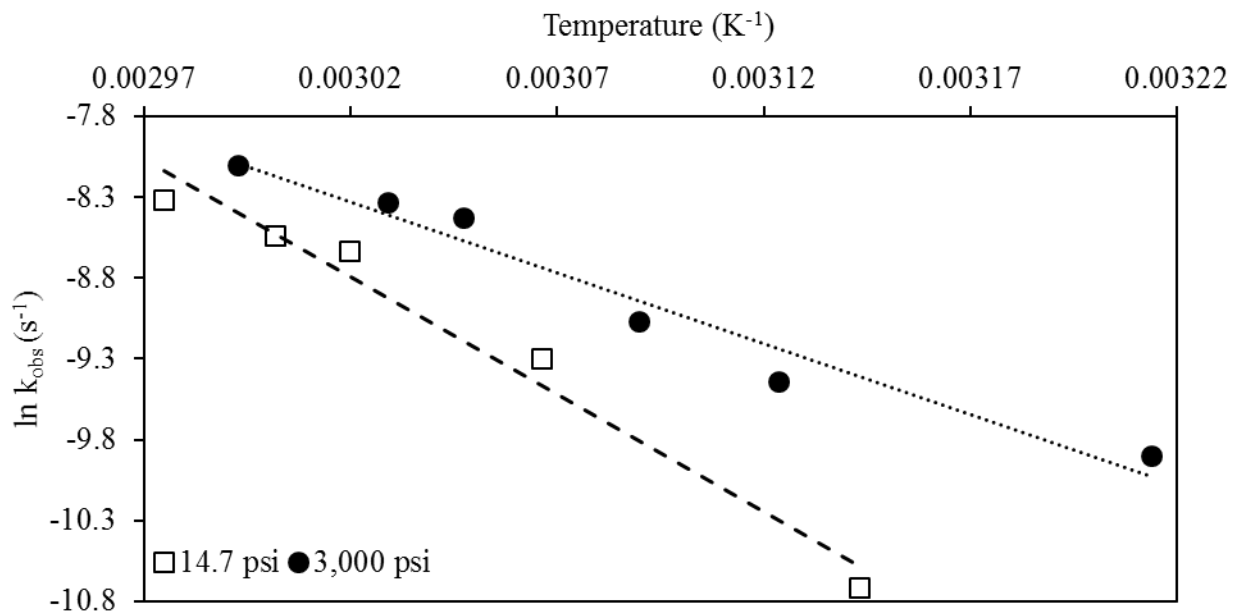


Figure 19. Activation energy for furfural removal with 0 and 3,000 psi applied to the reactor.

CHAPTER 6: Conclusions

Many compounds were identified in the hydraulic fracturing enzyme breaking LEB-10X. One compound of particular interest, furfural, was chosen to be studied because it is a well-known pollutant in many industries and has not been examined for oxidative remediation via activated persulfate. The main goal of this study was to assess the environmental risk of the interactions between hydraulic fracturing fluid components and sodium persulfate and help determine what chemical changes are taking place over the course of a fracture.

Furfural degradation was achieved by using sulfate radicals produced from persulfate activation through heat, iron, and acidification. The reaction rates were influenced by the solution temperature, initial pH, sodium persulfate dose, and iron concentration. The type of iron, Fe (II) or (III), added to solution had less of an impact of on reaction rate than these other factors. The results were promising, indicating that furfural pollution may be oxidized via persulfate and optimized for rapid ISCO. Adjusting solution pH to 2.54 decreased the activation energy of this reaction by at least 30%. The optimal conditions for ISCO of furfural using any dose of sodium persulfate are elevated temperatures, low pH, and ferric sulfate concentration up to 25 mg L⁻¹. The reaction byproducts were also identified and their transformation mechanisms were suggested.

Furfural degradation was further investigated in hydraulic fracturing fluids. It was shown that the presence of hydraulic fracturing brine increases the amount of time it takes to achieve a certain percentage of furfural removal. However, the reaction was still very dependent of solution temperature, pH, iron concentration, and persulfate dose. Furthermore, elevated pressure was determined to have an impact on furfural degradation via persulfate. Elevated pressures nearly halved the activation energy observed without any applied pressure. The changes in the reaction byproducts formed have important significance for environmental applications. Different types of DBPs were formed. Some of the byproducts are not very well studied, but others, such as bromoform, are known carcinogens and regulated by the EPA for drinking water treatment.

REFERENCES

1. Artusa, A., et al. *United States Drought Monitor*. 2016 May 24, 2016 [cited 2016 May 30]; Available from: <http://droughtmonitor.unl.edu/>.
2. Administration, U.E.I., *Annual Energy Outlook 2014 with Projections to 2040*. 2014, US Energy Information Administration Washington, DC, USA.
3. Spellman, F.R., *Environmental impacts of hydraulic fracturing*. 2012: CRC Press.
4. Smith, J.R., *Hydraulic Fracturing for Natural Gas Extraction: Research and Regulatory Impacts*. 2015.
5. Boudet, H., et al., “Fracking” controversy and communication: Using national survey data to understand public perceptions of hydraulic fracturing. *Energy Policy*, 2014. **65**: p. 57-67.
6. Nicot, J.-P. and B.R. Scanlon, *Water use for shale-gas production in Texas, US*. *Environmental science & technology*, 2012. **46**(6): p. 3580-3586.
7. Briskin, J., *Potential impacts of hydraulic fracturing for oil and gas on drinking water resources*. *Ground water*, 2014. **53**(1): p. 19-21.
8. Freyman, M., *Hydraulic fracturing & water stress: Water demand by the numbers*. Ceres, 2014: p. 49-50.
9. King, G.E. *Hydraulic fracturing 101: what every representative, environmentalist, regulator, reporter, investor, university researcher, neighbor and engineer should know about estimating frac risk and improving frac performance in unconventional gas and oil wells*. in *SPE Hydraulic Fracturing Technology Conference*. 2012. Society of Petroleum Engineers.
10. Howarth, R.W., A. Ingraffea, and T. Engelder, *Natural gas: Should fracking stop?* *Nature*, 2011. **477**(7364): p. 271-275.
11. Gregory, K.B., R.D. Vidic, and D.A. Dzombak, *Water management challenges associated with the production of shale gas by hydraulic fracturing*. *Elements*, 2011. **7**(3): p. 181-186.
12. Lauer, N.E., J.S. Harkness, and A. Vengosh, *Brine Spills Associated with Unconventional Oil Development in North Dakota*. *Environmental Science & Technology*, 2016. **50**(10): p. 5389-5397.
13. Colborn, T., et al., *Natural gas operations from a public health perspective*. *Human and ecological risk assessment: An International Journal*, 2011. **17**(5): p. 1039-1056.
14. Bamberger, M. and R.E. Oswald, *Impacts of Gas Drilling on Human and Animal Health*. *NEW SOLUTIONS: A Journal of Environmental and Occupational Health Policy*, 2012. **22**(1): p. 51-77.
15. Rahm, D., *Regulating hydraulic fracturing in shale gas plays: The case of Texas*. *Energy Policy*, 2011. **39**(5): p. 2974-2981.
16. Kreuze, A., C. Schelly, and E. Norman, *To frack or not to frack: Perceptions of the risks and opportunities of high-volume hydraulic fracturing in the United States*. *Energy Research & Social Science*.
17. Waxman, H.A., E.J. Markey, and D. DeGette, *Chemicals used in hydraulic fracturing*. United States House of Representatives Committee on Energy and Commerce Minority Staff, 2011.
18. Zoveidavianpoor, M. and A. Gharibi, *Application of polymers for coating of proppant in hydraulic fracturing of subterranean formations: A comprehensive review*. *Journal of Natural Gas Science and Engineering*, 2015. **24**: p. 197-209.

19. Liang, F., et al., *A comprehensive review on proppant technologies*. Petroleum, 2016. **2**(1): p. 26-39.
20. Dunlop, A.P., *Furfural Formation and Behavior*. Industrial & Engineering Chemistry, 1948. **40**(2): p. 204-209.
21. West, R.M., et al., *Carbon-carbon bond formation for biomass-derived furfurals and ketones by aldol condensation in a biphasic system*. Journal of Molecular Catalysis A: Chemical, 2008. **296**(1-2): p. 18-27.
22. Hoydonckx, H., et al., *Furfural and derivatives*. Ullmann's Encyclopedia of Industrial Chemistry, 2007.
23. Peters, F.N., *Industrial Uses of Furans*. Industrial & Engineering Chemistry, 1939. **31**(2): p. 178-180.
24. Xin-tong, L., *Application of the demulsification technique in petroleum refining*. Journal of Jilin Institute of Chemical Technology, 2011. **1**: p. 010.
25. Monlau, F., et al., *Do furanic and phenolic compounds of lignocellulosic and algae biomass hydrolyzate inhibit anaerobic mixed cultures? A comprehensive review*. Biotechnology Advances, 2014. **32**(5): p. 934-951.
26. Morris, J.A., A. Khettry, and E.W. Seitz, *Antimicrobial activity of aroma chemicals and essential oils*. Journal of the American Oil Chemists' Society, 1979. **56**(5): p. 595-603.
27. van der Pol, E.C., et al., *Identifying inhibitory effects of lignocellulosic by-products on growth of lactic acid producing micro-organisms using a rapid small-scale screening method*. Bioresource Technology, 2016. **209**: p. 297-304.
28. Castellino, N., O. Elmino, and G. Rozera, *Experimental research on toxicity of furfural*. Archives of Environmental Health: An International Journal, 1963. **7**(5): p. 574-582.
29. Occupational Safety and Health Guidelines for Furfural, U.O.S.a.H.A.O., Washington, DC, 1996.
30. Chen, H., *Lignocellulose Biorefinery Engineering: Principles and Applications*. 2015: Woodhead Publishing.
31. Sahu, A.K., et al., *Adsorption of furfural from aqueous solution onto activated carbon: Kinetic, equilibrium and thermodynamic study*. Separation Science and Technology, 2008. **43**(5): p. 1239-1259.
32. Sulaymon, A.H. and K.W. Ahmed, *Competitive Adsorption of Furfural and Phenolic Compounds onto Activated Carbon in Fixed Bed Column*. Environmental Science & Technology, 2008. **42**(2): p. 392-397.
33. Lucas, S., et al., *Adsorption isotherms for ethylacetate and furfural on activated carbon from supercritical carbon dioxide*. Fluid Phase Equilibria, 2004. **219**(2): p. 171-179.
34. Ranjan, R., et al., *Adsorption of fermentation inhibitors from lignocellulosic biomass hydrolyzates for improved ethanol yield and value-added product recovery*. Microporous and Mesoporous Materials, 2009. **122**(1-3): p. 143-148.
35. Gupta, P., et al., *The removal of furfural from water by adsorption with polymeric resins*. Separation Science and Technology, 2001. **36**(13): p. 2835-2844.
36. Anbia, M. and N. Mohammadi, *A nanoporous adsorbent for removal of furfural from aqueous solutions*. Desalination, 2009. **249**(1): p. 150-153.
37. Zhang, K., et al., *Removal of the Fermentation Inhibitor, Furfural, Using Activated Carbon in Cellulosic-Ethanol Production*. Industrial & Engineering Chemistry Research, 2011. **50**(24): p. 14055-14060.

38. Hoffman, F., *Ground - Water Remediation Using "Smart Pump and Treat"*. Ground Water, 1993. **31**(1): p. 98-106.
39. Tan, C., et al., *Heat-activated persulfate oxidation of diuron in water*. Chemical Engineering Journal, 2012. **203**: p. 294-300.
40. Liang, C.J., et al., *Thermally activated persulfate oxidation of trichloroethylene (TCE) and 1, 1, 1-trichloroethane (TCA) in aqueous systems and soil slurries*. Soil and sediment contamination: An international journal, 2003. **12**(2): p. 207-228.
41. Aliu, A.O., J. Guo, and S. Wang, *Hydraulic Fracture Fluid For Gas Reservoirs in Petroleum Engineering Applications Using Sodium Carboxy Methyl Cellulose as Gelling Agent*. Journal of Natural Gas Science and Engineering.
42. Cooper, J., L. Stamford, and A. Azapagic, *Environmental Impacts of Shale Gas in the UK: Current Situation and Future Scenarios*. Energy Technology, 2014. **2**(12): p. 1012-1026.
43. Navarrete, R.C., et al., *Experiments in Fluid Loss and Formation Damage with Xanthan-Based Fluids While Drilling*. Society of Petroleum Engineers.
44. Edwards, P.J., L.L. Tracy, and W.K. Wilson, *Chloride concentration gradients in tank-stored hydraulic fracturing fluids following flowback*. 2011.
45. Waldemer, R.H., et al., *Oxidation of chlorinated ethenes by heat-activated persulfate: kinetics and products*. Environmental Science & Technology, 2007. **41**(3): p. 1010-1015.
46. Kolthoff, I.M. and I.K. Miller, *The Chemistry of Persulfate. I. The Kinetics and Mechanism of the Decomposition of the Persulfate Ion in Aqueous Medium I*. Journal of the American Chemical Society, 1951. **73**(7): p. 3055-3059.
47. Liu, H., et al., *In Situ Chemical Oxidation of Contaminated Groundwater by Persulfate: Decomposition by Fe(III)- and Mn(IV)-Containing Oxides and Aquifer Materials*. Environmental Science & Technology, 2014. **48**(17): p. 10330-10336.
48. Liu, H., et al., *Oxidation of Benzene by Persulfate in the Presence of Fe(III)- and Mn(IV)-Containing Oxides: Stoichiometric Efficiency and Transformation Products*. Environmental Science & Technology, 2016. **50**(2): p. 890-898.
49. Zhao, D., et al., *Effect and mechanism of persulfate activated by different methods for PAHs removal in soil*. Journal of Hazardous Materials, 2013. **254–255**: p. 228-235.
50. Liang, C., et al., *Persulfate oxidation for in situ remediation of TCE. I. Activated by ferrous ion with and without a persulfate–thiosulfate redox couple*. Chemosphere, 2004. **55**(9): p. 1213-1223.
51. Samarghandi, M.R., et al., *Furfural removal from synthetic wastewater by persulfate anion activated with electrical current: energy consumption and operating costs optimization*. Der Pharma Chemica. **7**(7): p. 48-57.
52. Borghei, S. and S. Hosseini, *Comparison of furfural degradation by different photooxidation methods*. Chemical Engineering Journal, 2008. **139**(3): p. 482-488.
53. Faramarzpour, M., M. Vossoughi, and M. Borghei, *Photocatalytic degradation of furfural by titania nanoparticles in a floating-bed photoreactor*. Chemical Engineering Journal, 2009. **146**(1): p. 79-85.
54. Crimi, M.L. and J. Taylor, *Experimental evaluation of catalyzed hydrogen peroxide and sodium persulfate for destruction of BTEX contaminants*. Soil & Sediment Contamination, 2007. **16**(1): p. 29-45.

55. Yang, S., et al., *Degradation efficiencies of azo dye Acid Orange 7 by the interaction of heat, UV and anions with common oxidants: Persulfate, peroxymonosulfate and hydrogen peroxide*. Journal of Hazardous Materials, 2010. **179**(1–3): p. 552-558.
56. Zhao, D., et al., *Effect and mechanism of persulfate activated by different methods for PAHs removal in soil*. Journal of hazardous materials, 2013. **254**: p. 228-235.
57. Acero, J.L. and U.v. Gunten, *Influence of Carbonate on the Ozone/Hydrogen Peroxide Based Advanced Oxidation Process for Drinking Water Treatment*. Ozone: Science & Engineering, 2000. **22**(3): p. 305-328.
58. Campos-Martin, J.M., G. Blanco-Brieva, and J.L.G. Fierro, *Hydrogen Peroxide Synthesis: An Outlook beyond the Anthraquinone Process*. Angewandte Chemie International Edition, 2006. **45**(42): p. 6962-6984.
59. Li, R., et al., *Heterogeneous Fenton oxidation of 2,4-dichlorophenol using iron-based nanoparticles and persulfate system*. Chemical Engineering Journal, 2015. **264**: p. 587-594.
60. Legarth, B., E. Huenges, and G. Zimmermann, *Hydraulic fracturing in a sedimentary geothermal reservoir: Results and implications*. International Journal of Rock Mechanics and Mining Sciences, 2005. **42**(7–8): p. 1028-1041.
61. Barbot, E., et al., *Spatial and Temporal Correlation of Water Quality Parameters of Produced Waters from Devonian-Age Shale following Hydraulic Fracturing*. Environmental Science & Technology, 2013. **47**(6): p. 2562-2569.
62. Struchtemeyer, C.G. and M.S. Elshahed, *Bacterial communities associated with hydraulic fracturing fluids in thermogenic natural gas wells in North Central Texas, USA*. FEMS Microbiology Ecology, 2012. **81**(1): p. 13-25.
63. Liang, C., Z.-S. Wang, and N. Mohanty, *Influences of carbonate and chloride ions on persulfate oxidation of trichloroethylene at 20 °C*. Science of The Total Environment, 2006. **370**(2–3): p. 271-277.
64. Petri, B.G., et al., *Fundamentals of ISCO Using Persulfate*, in *In Situ Chemical Oxidation for Groundwater Remediation*, L.R. Siegrist, M. Crimi, and J.T. Simpkin, Editors. 2011, Springer New York: New York, NY. p. 147-191.
65. Bennedsen, L.R., J. Muff, and E.G. Sjøgaard, *Influence of chloride and carbonates on the reactivity of activated persulfate*. Chemosphere, 2012. **86**(11): p. 1092-1097.
66. Huie, R.E. and C.L. Clifton, *Rate constants for hydrogen abstraction reactions of the sulfate radical, SO₄⁻. Alkanes and ethers*. International Journal of Chemical Kinetics, 1989. **21**(8): p. 611-619.
67. Kiwi, J., A. Lopez, and V. Nadtochenko, *Mechanism and Kinetics of the OH-Radical Intervention during Fenton Oxidation in the Presence of a Significant Amount of Radical Scavenger (Cl⁻)*. Environmental Science & Technology, 2000. **34**(11): p. 2162-2168.
68. Snyder, S., *Water scarcity--the US connection*. African Journal of Food, Agriculture, Nutrition and Development, 2014. **14**(6): p. 14-15.
69. Devineni, N., et al., *America's water risk: Current demand and climate variability*. Geophysical Research Letters, 2015. **42**(7): p. 2285-2293.
70. Boyer, E.W., et al., *The impact of Marcellus gas drilling on rural drinking water supplies*. 2012.
71. Paugh, L.O. *Marcellus Shale Water Management Challenges in Pennsylvania*. in *SPE Shale Gas Production Conference*. 2008. Society of Petroleum Engineers.

72. Hickenbottom, K.L., et al., *Forward osmosis treatment of drilling mud and fracturing wastewater from oil and gas operations*. *Desalination*, 2013. **312**: p. 60-66.
73. Parker, K.M., et al., *Enhanced Formation of Disinfection Byproducts in Shale Gas Wastewater-Impacted Drinking Water Supplies*. *Environmental Science & Technology*, 2014. **48**(19): p. 11161-11169.
74. Harkness, J.S., et al., *Iodide, Bromide, and Ammonium in Hydraulic Fracturing and Oil and Gas Wastewaters: Environmental Implications*. *Environmental Science & Technology*, 2015. **49**(3): p. 1955-1963.
75. USEPA. *Stage 1 and Stage 2 Disinfectants and Disinfection Byproducts Rules*. [cited 2016 June 10]; Available from: <https://www.epa.gov/dwreginfo/stage-1-and-stage-2-disinfectants-and-disinfection-byproducts-rules#compliance>.
76. Lu, J., et al., *Transformation of bromide in thermo activated persulfate oxidation processes*. *Water Research*, 2015. **78**: p. 1-8.
77. Tan, J., et al., *Impact of bromide on halogen incorporation into organic moieties in chlorinated drinking water treatment and distribution systems*. *Science of The Total Environment*, 2016. **541**: p. 1572-1580.
78. Richardson, S.D., J.E. Simmons, and G. Rice, *Peer Reviewed: Disinfection Byproducts: The Next Generation*. *Environmental Science & Technology*, 2002. **36**(9): p. 198A-205A.
79. *Chemical Use In Hydraulic Fracturing*. 2016 [cited 2016 April 19]; Available from: <http://fracfocus.org/water-protection/drilling-usage>.
80. Leili, M., G. Moussavi, and K. Naddafi, *Degradation and mineralization of furfural in aqueous solutions using heterogeneous catalytic ozonation*. *Desalination and Water Treatment*, 2013. **51**(34-36): p. 6789-6797.
81. Nezamzadeh-Ejhi, A. and S. Moeinirad, *Heterogeneous photocatalytic degradation of furfural using NiS-clinoptilolite zeolite*. *Desalination*, 2011. **273**(2-3): p. 248-257.
82. Boopathy, R., H. Bokang, and L. Daniels, *Biotransformation of furfural and 5-hydroxymethyl furfural by enteric bacteria*. *Journal of Industrial Microbiology*, 1993. **11**(3): p. 147-150.
83. Wang, T., T. Kadlac, and R. Lenahan, *Persistence of fenthion in the aquatic environment*. *Bulletin of Environmental Contamination and Toxicology*, 1989. **42**(3): p. 389-394.
84. Kaur, I., et al., *Persistence of Endosulfan (Technical) in Water and Soil*. *Environmental Technology*, 1998. **19**(1): p. 115-119.
85. Badawy, M.I. and M.A. El-Dib, *Persistence and fate of methyl parathion in sea water*. *Bulletin of environmental contamination and toxicology*, 1984. **33**(1): p. 40-49.
86. Liang, C., C.-P. Liang, and C.-C. Chen, *pH dependence of persulfate activation by EDTA/Fe(III) for degradation of trichloroethylene*. *Journal of Contaminant Hydrology*, 2009. **106**(3-4): p. 173-182.
87. Rodriguez, S., et al., *Oxidation of Orange G by persulfate activated by Fe(II), Fe(III) and zero valent iron (ZVI)*. *Chemosphere*, 2014. **101**: p. 86-92.
88. Snoeyink, V.L. and D. Jenkins, *Water chemistry*. 1980: John Wiley.
89. Tsitonaki, A., et al., *In Situ Chemical Oxidation of Contaminated Soil and Groundwater Using Persulfate: A Review*. *Critical Reviews in Environmental Science and Technology*, 2010. **40**(1): p. 55-91.
90. Liang, C., Z.-S. Wang, and C.J. Bruell, *Influence of pH on persulfate oxidation of TCE at ambient temperatures*. *Chemosphere*, 2007. **66**(1): p. 106-113.

91. House, D.A., *Kinetics and Mechanism of Oxidations by Peroxydisulfate*. Chemical Reviews, 1962. **62**(3): p. 185-203.
92. Kolthoff, I., A. Medalia, and H.P. Raaen, *The Reaction between Ferrous Iron and Peroxides. IV. Reaction with Potassium Persulfate Ia*. Journal of the American Chemical Society, 1951. **73**(4): p. 1733-1739.
93. Xu, X.-R. and X.-Z. Li, *Degradation of azo dye Orange G in aqueous solutions by persulfate with ferrous ion*. Separation and Purification Technology, 2010. **72**(1): p. 105-111.
94. Anipsitakis, G.P., D.D. Dionysiou, and M.A. Gonzalez, *Cobalt-Mediated Activation of Peroxymonosulfate and Sulfate Radical Attack on Phenolic Compounds. Implications of Chloride Ions*. Environmental Science & Technology, 2006. **40**(3): p. 1000-1007.
95. Aiken, G.R., *Chloride interference in the analysis of dissolved organic carbon by the wet oxidation method*. Environmental Science & Technology, 1992. **26**(12): p. 2435-2439.
96. Barceló, D., *Emerging organic contaminants and human health*. Vol. 20. 2012: Springer.
97. USEPA. *Table of Regulated Drinking Water Contaminants*. [cited 2016 June 10]; Available from: <https://www.epa.gov/ground-water-and-drinking-water/table-regulated-drinking-water-contaminants>.
98. Stalter, D., et al., *Fingerprinting the reactive toxicity pathways of 50 drinking water disinfection by-products*. Water Research, 2016. **91**: p. 19-30.
99. Munch, D. and D. Hautman, *Method 551.1: Determination of Chlorination Disinfection Byproducts, Chlorinated Solvents, and Halogenated Pesticides/Herbicides in Drinking Water by Liquid-Liquid Extraction and Gas Chromatography with Electron-Capture Detection*. Methods for the Determination of organic compounds in drinking water, 1995.
100. Hladik, M.L., M.J. Focazio, and M. Engle, *Discharges of produced waters from oil and gas extraction via wastewater treatment plants are sources of disinfection by-products to receiving streams*. Science of The Total Environment, 2014. **466-467**: p. 1085-1093.

APPENDIX

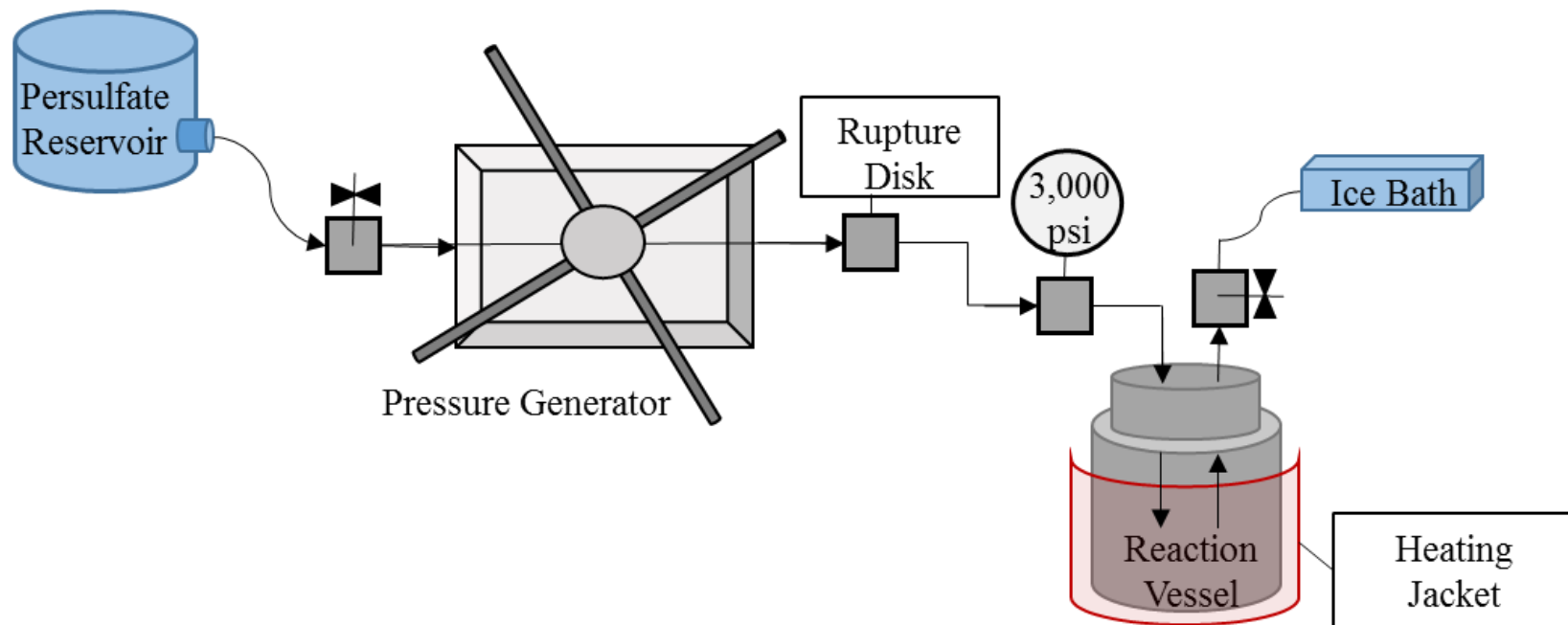


Figure A 1. Flow diagram of the pressurized reactor used in this study.



Figure A 2. Pressurized reactor set-up.

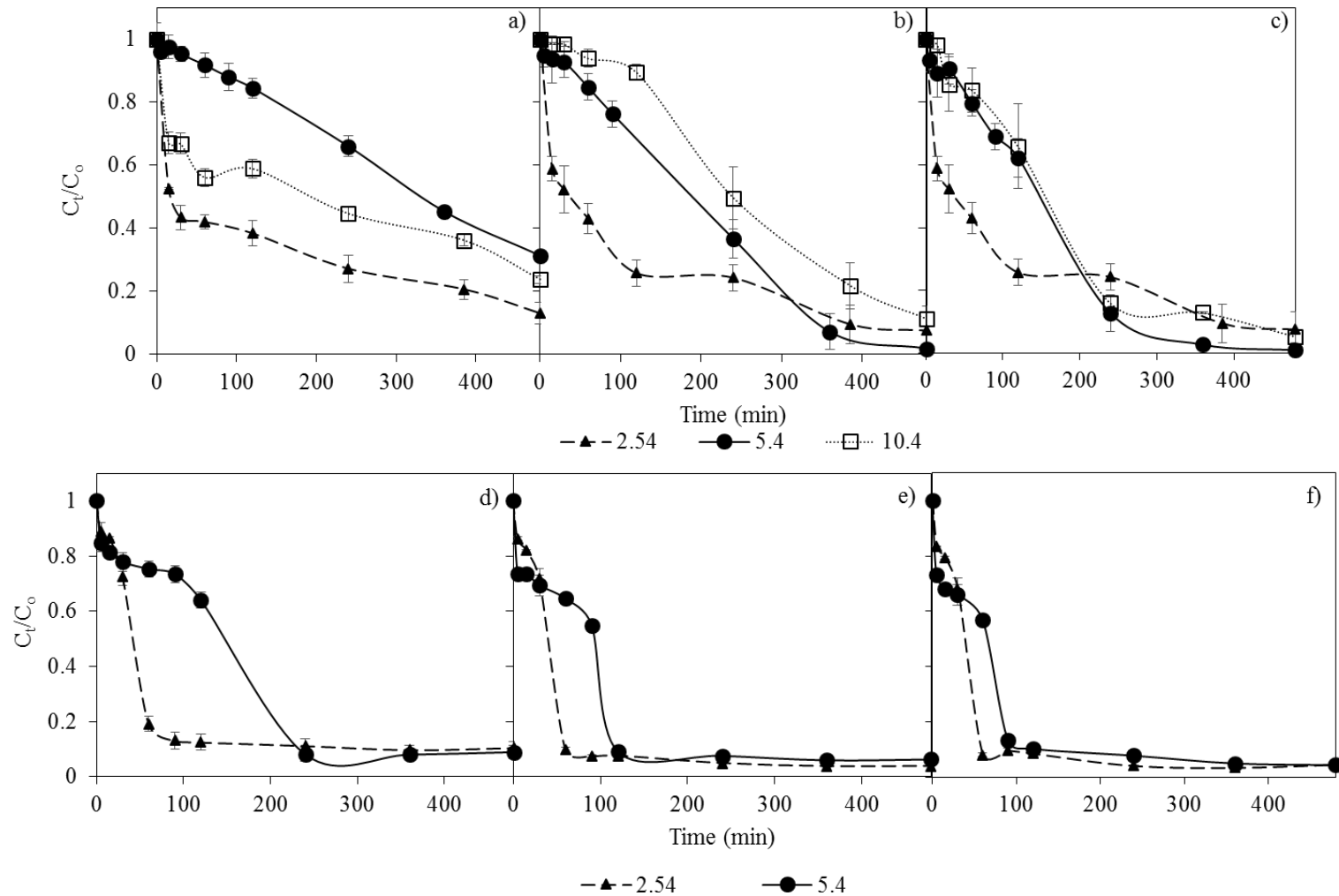


Figure A 3. The influence of varying pH on the degradation of furfural via persulfate oxidation with (a) 0 mg L⁻¹ ferric sulfate and 5 mM sodium persulfate, (b) 0 mg L⁻¹ ferric sulfate and 10 mM sodium persulfate, (c) 0 mg L⁻¹ ferric sulfate and 15 mM sodium persulfate, (d) 23.33 mg L⁻¹ ferric sulfate and 5 mM sodium persulfate, (e) 23.33 mg L⁻¹ ferric sulfate and 10 mM sodium persulfate, and (f) 23.33 mg L⁻¹ ferric sulfate and 15 mM sodium persulfate.

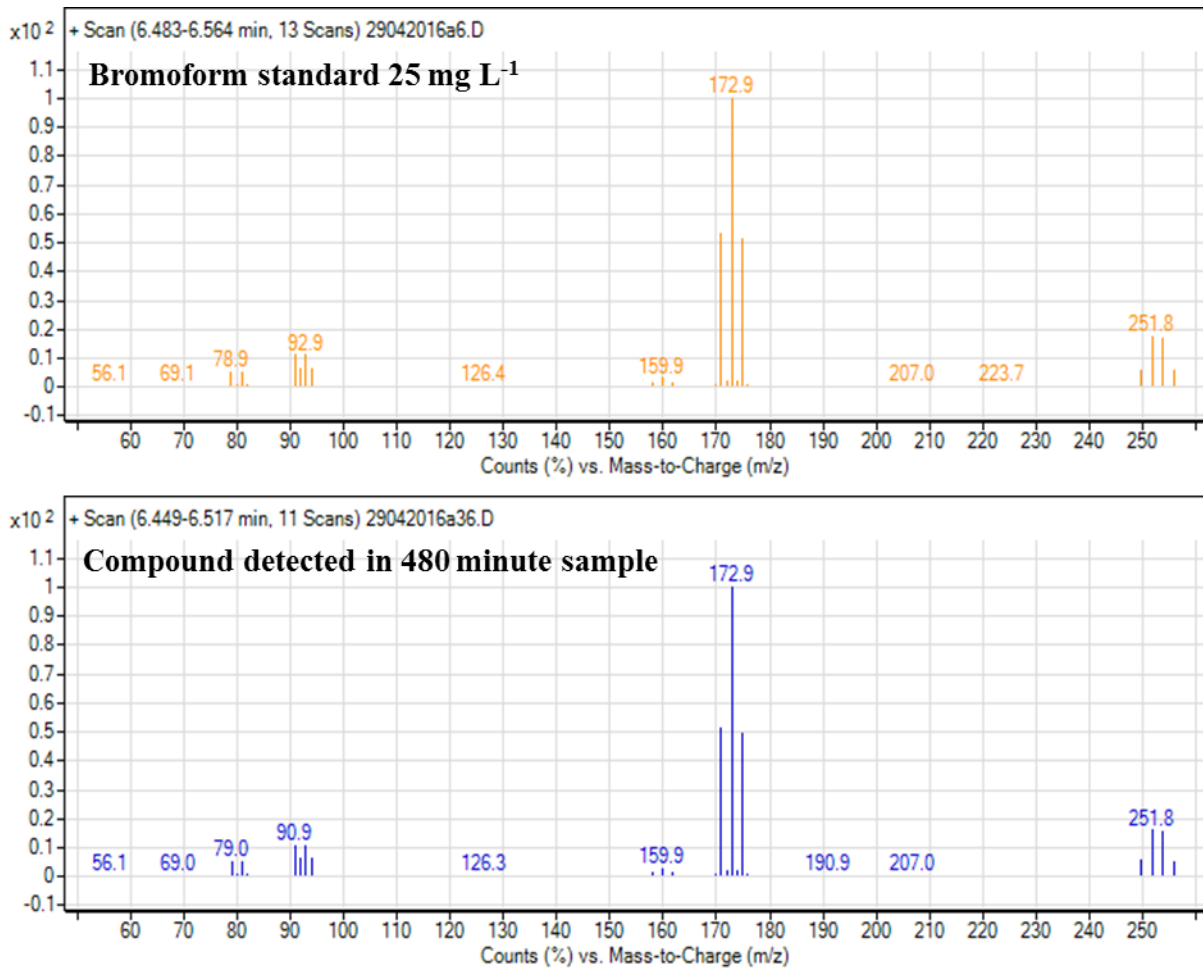


Figure A 4. Mass spectra of a bromoform standard and the bromoform detected in a hydraulic fracturing fluid sample.

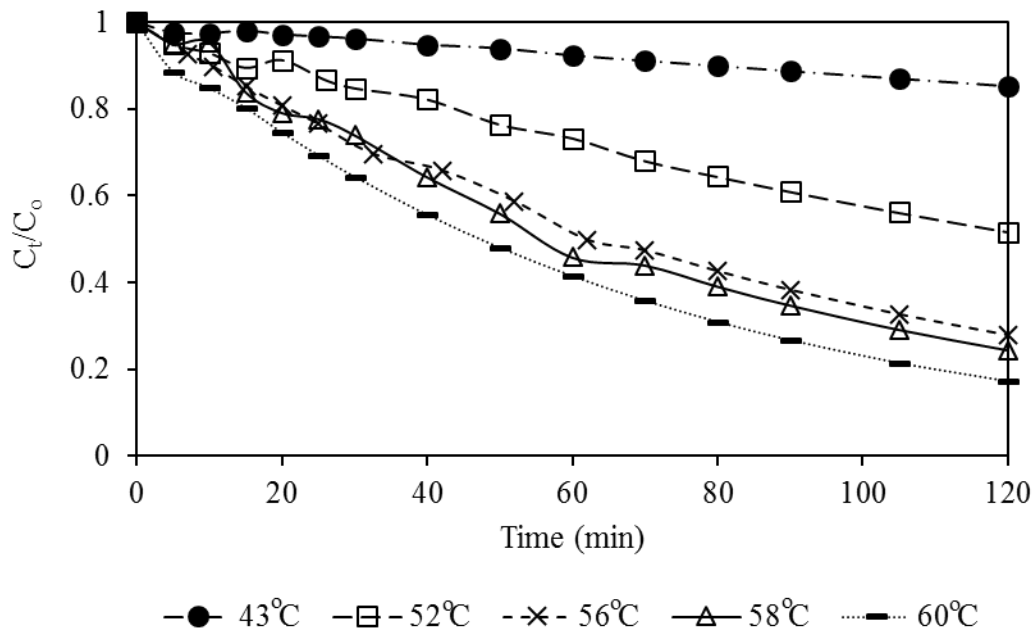


Figure A 5. Furfural removal over time in the high pressure reactor without applied pressure.

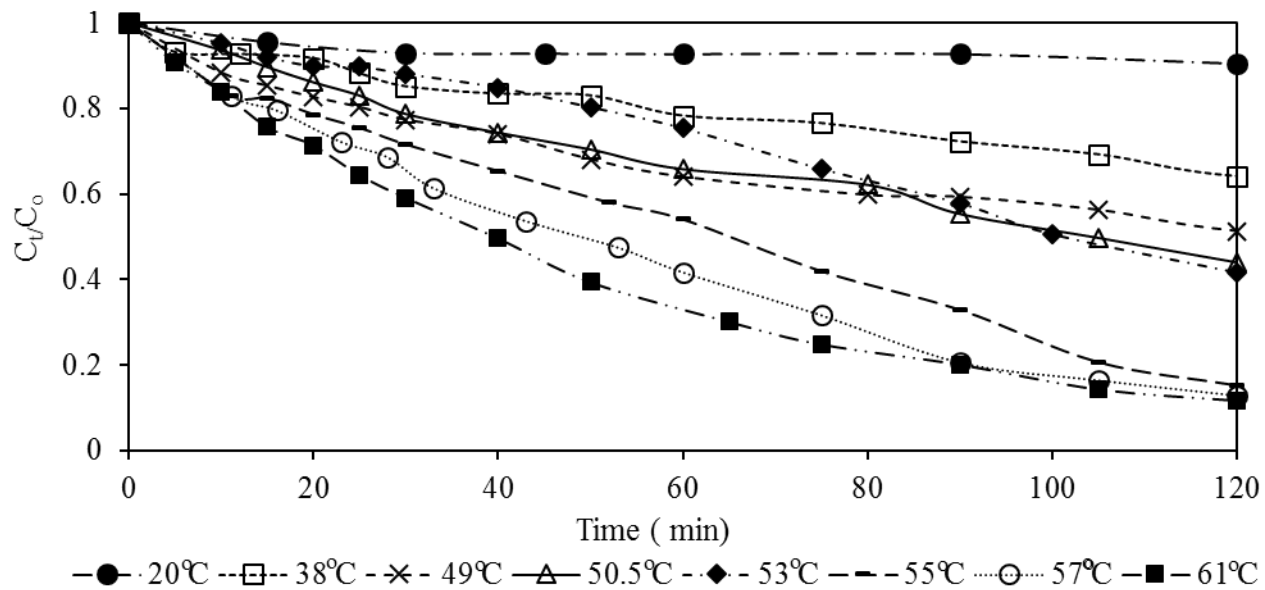


Figure A 6. Furfural removal over time in the high pressure reactor with 3,000 psi applied.

VITA

Katherine Manz earned a Bachelor's of Science degree in Chemistry from Rensselaer Polytechnic Institute (RPI) in Troy, NY in May 2013. During her time as an undergraduate, she performed research in Dr. K.V. Lakshmi's lab in the Baruch '60 Center for Biochemical Solar Energy Research. Her research focused on creating highly efficient and cost effective solar energy conversion through fundamental understanding of biological chemistry at the molecular level. For this research, she was awarded the John L. Marsh '58 RPI Summer Undergraduate Research Project Fellowship in 2011, the Arthur G. Schultz Award for Undergraduate Research in Chemistry in 2012, and an Undergraduate Research Project Fellowship for every semester from 2010 until 2013. She was also awarded the Who's Who Among Students in American Universities & Colleges at RPI. During the summer of 2012, Katherine was an undergraduate student research intern for the USDA NIFA CenUSA Bioenergy project at Iowa State University in Ames. Her project goals were to determine the expected net energy returns from the cellulosic systems of corn stover, switchgrass, and miscanthus and to compared the amounts of recoverable energy obtained from the crop systems.

At the University of Tennessee, Katherine is working with Dr. Kimberly Carter on the treatment of hydraulic fracturing fluids using Advanced Oxidation Processes (AOPs). She came to the University of Tennessee in Fall 2013 to pursue her Ph.D. in Energy Science and Engineering through the University of Tennessee, Knoxville and Oak Ridge National Laboratory's Bredesen Center for Interdisciplinary Research and Graduate Education. While working towards this goal, she earned her Master's of Science in Environmental Engineering in Sumer 2016. She will continue to finish her Ph.D. in Dr. Kimberly Carter's lab to further investigate the mechanism of disinfection byproduct formation in hydraulic fracturing fluids and engineering treatment processes that will eliminate the organic chemicals of hydraulic fracturing fluids may be reused for other purposes.